THE COMPLEX KOHN VARIATIONAL METHOD

T.N. Rescigno[1], C.W. McCurdy[2], A. E. Orel[3] and B.H. Lengsfield III[4]

[1]Physics Department, Lawrence Livermore National Laboratory
[2]National Energy Research Supercomputer Center
[3]Department of Applied Science, University of California Davis
Livermore, CA 94550
[4]IBM Almaden Research Center
San Jose, CA 95120

INTRODUCTION

Though substantial progress has been made in the theoretical study of electron collisions with molecules and molecular ions, most work has been restricted to diatomic or linear targets. Electron- and photon-molecule collision cross sections are needed in such diverse areas such as advanced laser development, pollution control, the design of high-speed space re-entry vehicles, the manufacture of semiconductor devices and plasma driven chemical synthesis. For example, the photoionization of polyatomic radicals, which plays an important role in combustion[1], requires a description of electron scattering from a polyatomic molecular ion. Such studies are scarce. In the area of plasma enhanced chemical vapor deposition and etching[2], studies indicate a subtle interplay between the neutrals, ions, electrons, and the surface. A critical lack of fundamental cross sections is hindering our understanding of these processes. Reliable theoretical methods are exceptionally important because of the extreme difficulty of experiments in this area.

Dissociative recombination of ions[3],

$$e^- + AB^+ \rightarrow A + B$$

plays an essential role in plasma dynamics, especially in low temperature plasmas, and also plays a major role in the operation of many excimer lasers.[4,5] For example, in the interstellar medium, the dissociative recombination of H_3^+ is an important contributor to the formation of hydrogen atoms and molecules[6]. For this simplest polyatomic dissociative recombination process, there is no adequate theory for very low collision energies and experiments have yielded cross sections that vary by orders of magnitude[7]. For these problems, there is additional complexity due to the coupling of the nuclear motion with the electron scattering. For diatomics, where the majority of work has been done, there is only one nuclear degree of freedom; even for a triatomic, three must be considered.

In addition to the practical interest, electron-polyatomic molecule collisions are of fundamental theoretical importance. With the many vibrational degrees of freedom and opportunities for interaction between excited electronic surfaces in several dimensions, it is clear that polyatomic targets offer a richer and more complex area of study than that found with diatomic targets. We have therefore been interested in developing a technology that is robust enough to study such polyatomic systems.

The complex Kohn method is an algebraic variational technique which, over the last few years, has been developed into a powerful approach for studying both heavy-particle (reactive) collisions[8] and electron scattering problems. It is somewhat surprising that although algebraic variational methods based on the Kato identity[9], such as the Kohn variational method[10] have been (and continue to be) used with much success in electron-atom problems[11], they received virtually no attention in molecular applications during the decade of the 1970's and were not developed in this connection until the mid 1980's. Two fundamental difficulties contributed to this neglect. One factor was the longstanding problem associated with the occurance of anomalous singularities in the reactance or K-matrices that made these techniques difficult to apply in large scale calculations[12]. The second problem concerns computational difficulties associated with the evaluation of multi-center integrals involving continuum functions.

The first problem can be trivially solved by formulating the variational problem with physical, outgoing wave (complex) boundary conditions, rather than the usual (real) standing-wave boundary conditions. This fact was originally used in nuclear physics by Mito and Kamimura[13], but went largely unnoticed until it was introduced into atomic and molecular physics by Miller and Jansen op de Haar in reactive heavy-particle scattering problems[14]. The connection between Miller's original work, the Kohn method and Kapur-Peierls theory was pointed out by McCurdy, Rescigno and Schneider[15] in 1987 and the complex Kohn method for electron-molecule scattering was developed over the ensuing few years.

A practical solution to the second problem required further theoretical developments. These included the judicious use of separable approximations to transfer the major burden of the problem to the construction and manipulation of bound-bound matrix elements[16]. Moreover, because the Kohn variational method is based on a Hamiltonian formulation of the collision problem, the full arsenal of bound-state structure methodology can be exploited in this connection. In order to evaluate the continuum matrix elements that are needed, we rely

on efficient 3-dimensional adaptive quadrature techniques[17,18]. This divorces the method from reliance on any specific analytic schemes and allows us considerable flexibility in choosing continuum basis functions.

The complex Kohn variational method is an efficient and flexible computational tool for studying electron-molecule scattering and molecular photoionization. We do not intend to give an exhaustive review of the many calculations which have been carried out with this method. Such a review can be found elsewhere[19]. Our purpose here is to provide a pedagical exposition of the technical aspects of the method. We will, however, site illustrative examples to highlight various aspects of the formulation. We should also point out that the fixed-nuclei electronic scattering problem, with which this review is mainly concerned, is only part of the full electron-molecule scattering picture. Much work centers on the nuclear motion problem, which is important in resonantly driven processes such as recombination and dissociative attachment[20], as well as near threshold vibrational and rotational excitation[21]. Meaningful (vibrationally and rotationally summed) cross sections can frequently be extracted solely from fixed-nuclei calculations. We will also show how the fixed-nuclei picture can be modified to provide threshold vibrational excitation cross sections. In many other cases the fixed-nuclei electronic problem can provide the input necessary to solve the full problem including the nuclear dynamics[22,23]. We will give one example of this for the case of dissociative recombination.

THEORETICAL FOUNDATION

The Kohn Variational Method for Neutral and Ionic Scattering

The basic concepts of the algebraic variational method are most easily illustrated for the case of scattering of a spinless particle by a spherically symmetric, short-range potential, V(r)[24]. We will therefore consider this problem in some detail before generalizing to the multichannel case and inelastic processes. Atomic units will be assumed throughout, unless otherwise stated. For the partial wave radial Schödinger equation, which we write as $Lu_\ell=0$, where

$$L = -\frac{1}{2}\frac{d^2}{dr^2} + \frac{\ell(\ell+1)}{2r^2} + \frac{Z}{r} + V(r) - \frac{k^2}{2} \quad , \tag{1}$$

we define the functional

$$L=\int_0^\infty u_\ell(r) L u_\ell(r) dr \quad . \tag{2}$$

The boundary conditions assumed for u_ℓ are

$$u_\ell(0) = 0$$

$$u_\ell(r) \underset{r\to\infty}{\sim} F_\ell(kr) + \lambda G_\ell(kr) \tag{3}$$

where F_ℓ and G_ℓ are two *linearly independent* solutions of the radial Schröedinger equation with V(r)=0. Their asymptotic normalization is, at this point, arbitrary. Note that Z/r is explicitly included in Eq. (1) so that we will be able to generalize to scattering by either neutral or ionic targets.

We now examine how L, which clearly vanishes when u_ℓ is an exact solution of the radial Schödinger equation, changes when the exact u_ℓ is replaced by a trial solution u_ℓ^t satisfying the same boundary conditions specified by Eq. (3), that is, with

$$\delta u_\ell(r) \equiv u_\ell^t(r) - u_\ell(r) \tag{4}$$

and

$$\delta u_\ell(0) = 0$$
$$\delta u_\ell(r) \underset{r\to\infty}{\sim} \delta\lambda G_\ell(r) \tag{5}$$

The result is

$$\delta L = \int_0^\infty \delta u_\ell L\, u_\ell dr + \int_0^\infty u_\ell L\, \delta u_\ell dr + \int_0^\infty \delta u_\ell L\, \delta u_\ell dr \tag{6}$$

Integrating the second term on the RHS of Eq. (6) by parts and making use of Eqs. (3) and (4) and the fact that $L\, u_\ell = 0$ gives

$$\delta L = -\frac{k}{2} W \delta\lambda + \int_0^\infty \delta u_\ell(r) L\, \delta u_\ell(r)\, dr \tag{7}$$

where W is the Wronskian defined by

$$W = F_\ell(x)\frac{d}{dx}G_\ell(x) - G_\ell(x)\frac{d}{dx}F_\ell(x)$$
$$= \text{constant} \tag{8}$$

Eq. (7), which is known as the Kato identity, expresses the exact value of λ in terms of the approximate value of the functional L and a term which is second order in the error in the wave function. The Kato identity thus provides a stationary principle for approximating λ:

$$\lambda^s = \lambda^t + \frac{2}{kW}\int_0^\infty u_\ell^t L\, u_\ell^t dr \quad . \tag{9}$$

Eq. (9) can be solved explicitly for a trial wave function that contains only linear trial coefficients. If we choose a trial function of the form

$$u_\ell^t = f_\ell(r) + \lambda^t g_\ell(r) + \sum_{i=1}^{n} c_i \varphi_i \tag{10}$$

where $\{\varphi_i\}$ are a set of square-integrable functions and

$$\begin{aligned} f_\ell(r) &\underset{r\to\infty}{\sim} F_\ell(kr) \\ g_\ell(r) &\underset{r\to\infty}{\sim} G_\ell(kr) \end{aligned} \quad , \tag{11}$$

then the coefficients λ^t and c_i are determined from the conditions:

$$\frac{\partial\lambda^s}{\partial c_i} = \frac{\partial\lambda^s}{\partial\lambda^t} = 0 \quad . \tag{12}$$

Substituting Eq. (10) into Eq. (9) and taking the derivative with respect to c_i gives

$$\int_0^\infty \varphi_i L\, u_\ell^t dr = 0 \quad , i = 1,,,n \quad . \tag{13}$$

Differentiation with respect to λ^t gives, after some rearrangement,

$$\int_0^\infty g_\ell L\, u_\ell^t dr = 0 \quad . \tag{14}$$

Eqs. (13) and (14) can be expressed in a compact form by relabeling the basis functions $g_\ell(r)$ and $\varphi_i(r)$ into a single set $\{\varphi_i\}$, $i=0,,,n$ with $\varphi_0 \equiv g_\ell$ and denoting the linear parameters $(\lambda^t, c_1,,,c_n\}$ by the vector $\mathbf{c}$. The result is:

$$\mathbf{c} = -\underline{M}^{-1}\, \mathbf{s} \tag{15}$$

where $\underline{M}$ is a matrix with elements

$$M_{ij} = \int_0^\infty \varphi_i L\, \varphi_j dr \quad , i,j = 0,,,n \tag{16}$$

and s is a vector with elements

$$s_i = \int_0^\infty \varphi_i L\, f_\ell dr \quad , i = 0,,,n \quad . \tag{17}$$

The *stationary* value of λ^s is obtained by substituting Eq. (15) into Eq. (9) to obtain:

$$\lambda^s = \frac{2}{kW}\left[\int_0^\infty f_\ell L\, f_\ell dr - sM^{-1}s\right] \quad . \tag{18}$$

We must now specify a form for the reference continuum functions F_ℓ and G_ℓ. We can take F_ℓ (and f_ℓ) to be the regular Coulomb function[25]. The traditional choice for G_ℓ is the irregular Coulomb function. The function g_ℓ, which must be regular at r=0, is usually obtained by multiplying G_ℓ by a suitable cut-off function that approaches unity for large r. With this choice, W=-1, λ is simply the tangent of the phase shift, $\tan\delta_\ell$, and Eq. (18) reduces to the familiar Kohn variational expression for $\tan\delta_\ell^s$. In the case of Coulomb scattering, δ_ℓ is of course the phase shift caused by the potential V(r) and does not include the Coulomb phase shift. When the continuum functions are so chosen, M is a real symmetric matrix and has zero determinant at the real values of E corresponding to the eigenvalues of H in the basis of φ_i plus g_ℓ. At these energies, Eq. (18) is singular; this is the origin of the so-called Kohn anomalies[12].

If g_ℓ is chosen to be an outgoing function $h_\ell^+(r)$, defined as

$$h_\ell^+(r) = i\,[\,F_\ell(kr) - i\,G_\ell(kr)]/\sqrt{k} \quad , \tag{19}$$

then W=-1/k and Eq. (18) becomes an expression for the T-matrix, $\lambda = T_\ell = e^{i\delta_\ell}\sin\delta_\ell$:

$$T_\ell^s = -2\left[\int_0^\infty f_\ell L\, f_\ell dr - sM^{-1}s\right] \quad . \tag{20}$$

M is now a complex symmetric matrix and *its inverse is generally nonsingular at real energies*[15]. We thus call this form of the variational equations the complex Kohn method. While M^{-1} can , in principle, be singular at a real energy, such an occurrence is improbable and is not a problem in practical calculations.

Continuum Basis Functions

The continuum basis functions used in a variational trial function must be regular at the origin. The traditional choice has been to use Ricatti-Bessel (or in the case of ionic targets, Coulomb-Bessel) functions, with a simple exponential cut-off applied to the irregular

solution. This choice was historically motivated by the desire to use simple functions that would not overly complicate the analytic evaluation of free-free integrals[26]. However, in our implementation of the method, we do not rely on any specific analytic schemes and thus have considerable flexibility in choosing continuum basis functions. Moreover, since we found in early applications that there could be quite a bit of sensitivity to the traditional cut-off, we were led to seek to a more physical choice for regularizing the outgoing wave continuum basis functions[27]. The choice we made was inspired by the work of Sun et al.[28] on the Kohn and generalized Newton variational principles.

The outgoing continuum function we employ is defined as:

$$g_\ell(r) = A\, G_\ell^+\, VF_\ell \quad , \tag{21}$$

where G_ℓ^+ is the radial partial wave free particle Green's function,

$$G_\ell^+(r,r') = \begin{matrix} -2/kF_\ell(kr)h_\ell^+(kr') & , & r \le r' \\ -2/kF_\ell(kr')h_\ell^+(kr) & , & r > r' \end{matrix} \quad , \tag{22}$$

V is any suitable "test potential' (we use a simple exponential) and the constant A is introduced in order to normalize g_ℓ (r) as in Eq. (19) and is thus given by

$$A = \left[2 \int_0^\infty F_\ell V F_\ell dr \right]^{-1} \tag{23}$$

The function g_ℓ is easily calculated by noting that it satisfies the inhomogeneous differential equation

$$\left(\frac{d^2}{d\rho^2} - \frac{\ell(\ell+1)}{\rho^2} - \frac{2Z}{k\rho} + 1 \right) g_\ell(\rho) = 2AVF_\ell(\rho) \tag{24}$$

It is a simple matter to construct the function required in Eq. (21) as a linear combination of a solution to Eq. (24) obtained by numerical integration and a solution of the corresponding homogeneous equation. This technique has the added advantage of not requiring the irregular function G_ℓ on the integration mesh[27].

Trial Wave Function for Electron-Molecule Scattering

To implement the complex Kohn method for electron-molecule scattering, we must generalize the simple trial function previously discussed to a form appropriate for multichannel scattering. We will use body-frame coordinates within the framework of the fixed-nuclei approximation. We write:[29]

$$\Psi_{\Gamma_0} = \sum_{\Gamma} A\left(\chi_{\Gamma} F_{\Gamma\Gamma_0}\right) + \sum_{\mu} d_{\mu}^{\Gamma_0} \Theta_{\mu} \quad . \tag{25}$$

The first sum runs over a set of energetically open N-electron target states, χ_Γ, and $F_{\Gamma\Gamma_0}$ is a one-electron function that describes the scattered electron. The index Γ_0 labels a particular degenerate solution corresponding to the initial state of the target and the operator A antisymmetrizes the orbital functions $F_{\Gamma\Gamma_0}$ into the functions χ_Γ. Note that we are using the symbol Γ to label all the quantum numbers needed to represent a physical state of the composite system, that is, the internal state of the target and the angular momentum of the scattered electron.The target functions χ_Γ may be single or multiconfiguration descriptions of the bound states of the molecule. It is assumed that $F_{\Gamma\Gamma_0}$ is, by construction, orthogonal to all the orbital functions used to construct χ_Γ. We use average natural orbital techniques to insure that the orbital space used to generate these states is kept manageably small. The functions Θ_m are a set of (N+1)-electron configuration state functions, (CSF's) orthogonal to the terms in the first sum of Eq. (25), constructed from square-integrable (Cartesian Gaussian) functions.

In general, the (N+1)-electron CSF's can be classified as one of three distinct types[30]. First, this sum contains the so-called 'penetration' terms, which relax any constraint implied by requiring $F_{\Gamma\Gamma_0}$ to be orthogonal to the orbitals used to build the χ_Γ[29]. Thus, these CSF's are built entirely from target orbitals. A second class of terms is possible in the case that multiconfiguration target states are used. Since the χ_Γ are then constructed as fixed linear combinations of CSF's, there will be an orthogonal complement of target states, presumed to be energetically closed, that uses the same CSF's in different linear combinations. These "CI relaxation terms" are built as the direct product of these other states and a square-integrable orbital. Finally, we can include other closed channels by constructing terms which are the direct product of a bound orbital and a disjoint set of target configurations (to be compared to CI-relaxation terms, which use the same set of CSF's as the open channel states). We refer to this latter set of CSF's as polarization terms. Both types of closed-channel contributions are necessary to describe the polarization and correlation effects that can dominate the scattering cross sections at low energy[31]. Note that these closed-channel contributions to the wave function fall off exponentially as any electron coordinate tends to infinity. This form of the trial function, which is often referred to as a close-coupling plus correlation (CCPC) expansion, is quite general and common to many closed-coupling formulations[32].

In algebraic variational methods such as the complex Kohn method, $F_{\Gamma\Gamma_0}$ is further expanded as

$$F_{\Gamma\Gamma_0} = \sum_{i} c_i^{\Gamma_0} \varphi_i + \sum_{\ell m} [f_\ell^\Gamma(k_r r)\delta_{\ell\ell_0}\delta_{mm_0}\delta_{\Gamma\Gamma_0} + T_{\ell\ell_0 mm_0}^{\Gamma\Gamma_0} g_\ell^\Gamma(k_r r)] Y_{\ell m}(\hat{r}) / r \tag{26}$$

where the φ_i are a set of square-integrable functions, $Y_{\ell m}$ is a normalized spherical harmonic and the functions f_ℓ^Γ and g_ℓ^Γ are the regular and outgoing-wave continuum

functions discussed in the previous section. This is the generalization of Eq. (10) to the multichannel case. The channel momenta k_Γ are determined by energy conservation,

$$k_\Gamma^2 / 2 = E - E_\Gamma \quad , \tag{27}$$

where E is the total energy of the composite system and E_Γ is the energy of the target molecule corresponding to state χ_Γ. The coefficients $T^{\Gamma\Gamma_0}_{\ell\ell_0 mm_0}$ are elements of the T-matrix and are the fundamental dynamical quantities from which differential and integral cross sections are constructed. In order to simplify the notation in what follows, we will adopt the convention of using $f^\Gamma_{\ell m}$ (or $g^\Gamma_{\ell m}$) to denote the product of a radial function f^Γ_ℓ (or g^Γ_ℓ) and $Y_{\ell m}/r$.

In principle, the total wave function can be described to any desired level of accuracy with a trial wave function of the form just outlined. In practice, the open-channel expansion is usually truncated rather severely and the target states themselves are approximate; we will see that the consequences of these two facts can profoundly effect the quality of the computed cross sections and that it will be very important to balance correlation effects in the N- and (N+1)- electron systems in the process of deciding what types of terms are reasonable to include in the trial wave function. We will return to these physical considerations later, but now we continue with the mechanics of how the variational equations are constructed and solved.

Feshbach Partitioning

It is convenient to partition the total wave function into two parts, $P\Psi_{\Gamma_0}$ and $Q\Psi_{\Gamma_0}$, corresponding to the two sums defined in Eq. (25). As we previously stated, the channel orbitals $F_{\Gamma\Gamma 0}$ which appear in $P\Psi_{\Gamma_0}$ are expanded as linear combinations of bound and continuum functions. These basis functions can be mutually orthogonalized without changing the resulting T-matrix, a property known as *transfer invariance*[11]. We will show later how this property can be exploited to simply the calculation of certain matrix elements. We also follow the common practice of requiring the channel orbitals to be orthogonal to all the bound-state orbitals which are used to form the target wave functions, and have commented that these additional constraints, if necessary, can be relaxed by including appropriate penetration terms in $Q\Psi_{\Gamma_0}$[33,34].

$P\Psi_{\Gamma_0}$ contains the asymptotic parameters from which collision cross sections are determined; since $Q\Psi_{\Gamma_0}$ is square-integrable, it is not explicitly needed for the determination of scattering parameters. In calculations which include the effect of closed channels, the set of Q-space configurations can become quite large. For this reason, and because of the fact that the configuration state functions $\{\Theta m\}$ are built solely from square-integrable orbitals, there are cases where it desirable to use bound-state molecular structure methods to treat the Q-space portion of the problem. However, there are applications, such as photoionization[35], in which the entire wave function, $P\Psi_{\Gamma_0} + Q\Psi_{\Gamma_0}$, is required to calculated a desired property. In such cases, Feshbach partitioning may not be the most efficient way to proceed.

Feshbach partitioning[36] is accomplished by formally solving the Schrödinger equation for $Q\Psi_{\Gamma_o}$ and then substituting the result into the equation for $P\Psi_{\Gamma_o}$. Defining M as H-E, we can derive in the usual way a modified Hamiltonian that determines $P\Psi$:

$$\begin{aligned} H_{eff} &= H_{PP} - M_{PQ} M_{QQ}^{-1} M_{QP} \\ &= H_{PP} - V_{opt} \end{aligned} \tag{28}$$

where MQQ^{-1} is the inverse of the Hamiltonian matrix spanned by the functions $\{\Theta m\}$. This allows us to drop the variational coefficients $d_\mu^{\Gamma_o}$ in Eq. (25) from further consideration. Note that the optical potential, V_{opt}, that we have defined is technically not the same as the Feshbach optical potential[36]. The difference lies in the fact that our $Q\Psi_{\Gamma_o}$ can contain orthogonality relaxing "penetration terms", in which case $Q\Psi_{\Gamma_o}$ will contain a portion of the open-channel wave function.

We can now proceed to use the effective Hamiltonian defined in Eq. (28) to define a functional, just as we did in the single-channel case, for the purpose of getting a stationary approximation to the T-matrix. The multichannel T-matrix can again be characterized as the stationary value of the Kohn functional

$$T_s^{\Gamma\Gamma'} = T_t^{\Gamma\Gamma'} - 2\int P\Psi_\Gamma (H_{eff} - E) P\Psi_{\Gamma'} \cdot dr_1 .. dr_{N+1} \tag{29}$$

By following the same procedures outlined in the single-channel case, we obtain the generalization of Eq. (20):

$$T_s = -2 \left(M_{00} - M_{q0}^t M_{qq}^{-1} M_{q0} \right) \tag{30}$$

where we have used a condensed matrix notation, in which open-channel indices are suppressed. The index 0 denotes the subspace spanned by the functions $\{\chi_\Gamma f_{\ell m}^\Gamma\}$ and the index q refers to the subspace spanned by $\{\chi_\Gamma g_{\ell m}^\Gamma\}$ and $\{\chi_\Gamma \varphi_i\}$. M refers to the operator H_{eff}-E. For example, the elements of M_{00} are defined as

$$(M_{00})_{\ell m \ell' m'}^{\Gamma\Gamma'} = \int A \left(\chi_\Gamma f_{\ell m}^\Gamma \right) (H_{eff} - E) A \left(\chi_{\Gamma'} f_{\ell' m'}^{\Gamma'} \right) dr_1 .. dr_{N+1} \tag{31}$$

and M_{q0} and M_{qq} are defined similarly.

The matrix M is thus built from elements that can be classified as either free-free, bound-free or bound-bound, depending upon whether two, one or zero continuum orbitals appear in the expression. The bound-bound terms, which generally constitute the largest class of matrix elements, can be evaluated using bound-state structure methodology. The bound-free and free-free terms must be handled numerically. Since the methods employed in evaluating these various Hamiltonian matrix elements are quite different, it is critical that we have some way of guaranteeing a consistent set of definitions for defining and ordering CSF's and establishing phase conventions. We will discuss the bound-bound problem first.

The effective Hamiltonian defined by Eq. (28) is an (N+1)-electron operator in a product space labelled by open channel target states. Operationally, we must reduce this many-electron operator to a matrix of one-electron operators defined over the functions used to expand $F_{\Gamma\Gamma_0}$ by integrating out the N coordinates of the target. The construction of the optical potential also requires the manipulation of operators built from (N+1)-electron Q-space configurations which are not in general labeled by target channels. The Q-space configurations of the "penetration" type are built entirely from target orbitals, while the relaxation and polarization configurations can involve both target and scattering orbitals. The insurance of consistency between the N-electron and (N+1)-electron problems with respect to phase conventions, ordering of configurations etc. may be difficult with molecular structure codes which make provision for automatic generation of configurations since these conventions may not be transparent. To avoid any possible ambiguity, we determine the target CI coefficients from a pseudo-(N+1)-electron CI calculation in which a *single* orbital is used to represent the scattered electron. Let $\{\Phi_i\}$, i=1,,n denote the N-electron configurations used to expand the target eigenstates. We first set up an n×n Hamiltonian in the (N+1)-electron space where each configuration is a direct product of a Φ_i and the single square-integrable function, φ_s. However, before carrying out this CI calculation, all one- and two-electron integrals involving φ_s are set to zero. Because there is no interaction between φ_s and the remaining N electrons, the diagonalization of this Hamiltonian will produce the desired N-electron target states. This set of target vectors can serve as prototypes for building a new set of vectors for use in the full (N+1)-electron problem in which a Hamiltonian is built from repeated products of the target configurations $\{\Phi_i\}$ and all the scattering orbitals in succession, $\{\varphi_j\}$,j=1,,p. Penetration and polarization configurations, which are denoted by Θ_q, are appended to the end of this list. This prototyping scheme removes any possible inconsistencies between the N- and (N+1)-electron problems and preserves the phase conventions used in the original determination of the target states. The procedure can also be modified if we wish to take specific account of the symmetry of the various open-channel target states. In that case, we would first group the target CSF's into different symmetry classes and then use a different prototype orbital, φ_s^{Λ}, for each class in order to couple up to a specific total symmetry, Λ.

The Q-space configurations, from which the optical potential is built, consist of the penetration and polarization terms explicitly included as Θ_q, and the CI relaxation terms to which we now turn our attention. Since the P-space vectors are constructed as direct products of scattering orbitals and a *fixed* number, m, of eigenstates of an $n \times n$ Hamiltonian matrix, the complement of P-space consists of the direct product of the scattering orbitals and the remaining(n-m) target eigenstates, which are presumed to be energetically closed. However, the algorithm that we use to include the CI relaxation terms in Q-space does <u>not</u> require the determination of all of the eigenvectors of the target Hamiltonian. Rather, we employ projection operators to account for these terms and can thereby avoid the explicit construction of H_{QQ}. We express H_{QQ} in a configuration state function basis rather than in the basis of CI eigenfunctions[37]:

$$
\begin{aligned}
H_{QQ} &= \begin{bmatrix} 1-|c_p\rangle\langle c_p| & 0 \\ 0 & 1 \end{bmatrix} \begin{bmatrix} H_{ij}^{kl} & H_{iq}^{k} \\ H_{iq}^{k\dagger} & H_{qq} \end{bmatrix} \begin{bmatrix} 1-|c_p\rangle\langle c_p| & 0 \\ 0 & 1 \end{bmatrix} \\
&\equiv \rho_Q H_{QQ}^{CSF} \rho_Q
\end{aligned}
\tag{32}
$$

where we have used the notation

$$
H_{ij}^{kl} = \langle \Phi_i \varphi_k | H | \Phi_j \varphi_l \rangle \quad , \tag{33}
$$

and c_p is a matrix built from the m open-channel eigenstates

$$
c_p = \begin{bmatrix} c_1^1 \cdots c_1^m & & & \\ & \ddots & & 0 \\ c_n^1 \quad c_n^m & & & \\ & \ddots & \ddots & \\ & & c_1^1 \quad c_1^m & \\ & 0 & & \\ & & c_n^1 \quad c_n^m & \end{bmatrix} \quad . \tag{34}
$$

where the number of replications of the n×m matrix c_j^i, which specifies the target state expansion coefficients, is determined by the number of scattering orbitals.

In building the optical potential defined by Eq. (28), H_{QQ} is used to solve a set of linear equations,

$$
(E - H_{QQ}) X_{QP} = H_{QP} \tag{35}
$$

and

$$
V_{PP}^{OPT} = H_{PQ} X_{QP} = H_{PQ} (E - H_{QQ})^{-1} H_{QP} \tag{36}
$$

The linear equations, Eq. (35), are solved iteratively by successively multiplying ($E-H_{QQ}$) by a set of trial vectors, (X^i, i=1, ··r) and solving a small set of linear equations in the trial space until convergence is achieved. This type of algorithm has been discussed in a number of papers and a detailed description will not be given here[38]. We only note that neither the projection operator, ρ_Q, nor the Q-space Hamiltonian, H_{QQ}^{CSF} , need be explicitly constructed[37]. A direct-CI procedure can be used to perform the multiplication of $(E - H_{QQ}^{CSF})$ times the projected trial function. This is a standard procedure in most modern electronic structure packages and allows us to employ large Hamiltonian matrices in the scattering calculations[39]. In cases where Q-space is very large, the procedure just outlined for obtaining V_{opt} will be for more efficient than explicitly inverting ($E-H_{QQ}$).

APPROXIMATION SCHEMES

Primitive Separable Expansions

The techniques of bound-state electronic structure theory can be used to evaluate bound-bound matrix elements; the matrix elements involving continuum basis functions are more problematic and the principal difficulty of any molecular scattering calculation is their evaluation. There are two critical steps that make this problem tractable for polyatomics. The first step, which we will now discuss, uses separable approximations to eliminate an entire class of continuum exchange and optical potential matrix elements[16]. The second step, which we take up in the following section, is the development of an efficient numerical technique for evaluating the remaining continuum matrix elements.

There are several ways to achieve a separable representation of an operator. In this discussion, we confine ourselves to what is sometimes referred to as a primitive separable representation of an operator which is obtained by its projection onto a finite basis[40]:

$$H \approx \sum_{\alpha\beta} |\varphi_\alpha > H_{\alpha\beta} < \varphi_\beta| \quad . \tag{37}$$

With reference to the effective Hamiltonian defined in Eq. (28), this type of representation is invoked for the exchange components of H_{PP}, as well as V_{opt}. The basis we use for this separable representation is the set of target orbitals, along with the square-integrable functions used to expand the channel orbitals $F_{\Gamma\Gamma_0}$. To see the usefulness of such representations, consider the expansion of the channel functions $F_{\Gamma\Gamma_0}$ given in Eq. (26). If we were to add any multiple of the square-integrable basis functions φ_i to the continuum functions f_ℓ^Γ and g_ℓ^Γ, the asymptotic form of $F_{\Gamma\Gamma_0}$ would of course remain unchanged. The process simply transfers a square-integrable term from the first sum to the second. We have already mentioned that the Kohn variational equations have the property of *transfer invariance* which means that the T-matrix elements are invariant to such a transformation[11]. We have formulated the Kohn variational equations with a strong orthogonality condition between the continuum basis functions and both the scattering orbitals, φ_i, as well as the orbitals used to construct the target wave functions. (Remember, we add penetration terms to relax any constraints implied by "target orthogonality" [29,33,34].)

Now consider a continuum matrix element, for example, a free-free matrix element of the type defined in Eq. (31). It is useful to separate this integral into a direct component,

$$\begin{aligned} {}^{\text{Direct}}(M_{00}^{PP})_{\ell m \ell' m'}^{\Gamma\Gamma'} &\equiv \int \chi_\Gamma(r_1 .. r_N) f_{\ell m}^{\Gamma}(r_{N+1}) \left(H_{pp} - E\right) \\ &\times \chi_{\Gamma'}(r_1 .. r_{N+1}) f_{\ell' m'}^{\Gamma'}(r_{N+1}) \; dr_1 .. dr_{N+1} \end{aligned} \tag{38}$$

and an exchange component arising from the interchange of "bound" and "free" electron coordinates. The short-range character of the exchange operators allows for their expansion in a rapidly convergent series of separable terms[16,40]. In the present context, the separable expansion of exchange terms leads to a great simplification. Indeed, if the exchange operators

are projected onto a finite set of (N+1)-electron configurations, Λ_m, which are made up from the entire set of target plus scattering square-integrable basis orbitals, then all free-free and bound-free exchange integrals will simply vanish. This is a consequence of the strong orthogonality condition we have imposed on the continuum functions, ie.

$$
\begin{aligned}
{}^{\text{Exchange}}\left(M_{00}^{pp}\right)_{\ell m \ell' m'}^{\Gamma\Gamma'} \approx & \sum_{m,n} \left\langle A\left(\chi_\Gamma f_{\ell m}^{\Gamma}\right) | \Lambda_m \right\rangle \\
& \times \left\langle \Lambda_m | \left(H_{pp} - E\right) | \Lambda_n \right\rangle \left\langle \Lambda_n | A\left(\chi_{\Gamma'} f_{\ell' m'}^{\Gamma'}\right) \right\rangle \\
& = 0
\end{aligned}
\tag{39}
$$

since $\left\langle \Lambda_n | A\left(\chi_{\Gamma'} f_{\ell' m'}^{\Gamma'}\right) \right\rangle = 0$. The presumption is that since the exchange interactions are relatively short-ranged, the square-integrable basis can be made large enough to make this a good approximation. Similarly, matrix elements involving continuum functions and (N+1)-electron CSF's are also expanded in a square-integrable bases:

$$
\begin{aligned}
\left\langle A\left(\chi_\Gamma f_{\ell m}^{N}\right) | (H-E) | \Theta \right\rangle \approx & \\
& \sum_m \left\langle A\left(\chi_\Gamma f_{\ell m}^{\Gamma}\right) | \Lambda_m \right\rangle \left\langle \Lambda_m | (H-E) | \Theta \right\rangle \\
& = 0
\end{aligned}
\tag{40}
$$

The consequence of these approximations is that no continuum matrix elements involving either exchange or optical potential interactions need be constructed and the entire effect of these interactions is carried in the bound-bound portions of the Hamiltonian. Whether or not this is a good approximation depends upon how many functions we include in the underlying L^2 basis and how close it comes to being complete for the purpose of representing the operators in question. In this context, one must bear in mind that the orbitals used in the determination of target wave functions must necessarily be excluded from the set of L^2 functions used to expand the channel scattering functions. There is no formal difficulty here, since these target orbitals, as we have stated, appear in appropriate (N+1)-electron "penetration" terms in Q-space. However, because the optical potential is only represented in separable form, the transference of terms from P-space to Q-space does involve an approximation. For this reason, we try to keep the target orbital space as compact as possible.

Adaptive Quadrature

We now turn our attention to the evaluation of the direct continuum integrals. Because the integrands can involve long-range multipole interactions, they are very difficult to converge by using separable expansions, so we handle these terms numerically. The first step is to write the direct integrals in terms of one-particle transition potentials. For example, we can write

$$\left\langle A(\chi_i f)|(H-E)|A(\chi_j g)\right\rangle_{direct} = \delta_{ij}\left\langle f|-1/2\nabla^2+E_i-E+V_{nuc}|g\right\rangle+\left\langle f|V_{ij}|g\right\rangle \tag{41}$$

where V_{ij} is the direct potential associated with the $i \rightarrow j$ transition:

$$V_{ij}(r) = \sum_{q=1,N} \int \chi_i(\hat{r}_1 .. \hat{r}_N) \frac{1}{|\vec{r}-\vec{r}_q|} \chi_j(\hat{r}_1 .. \hat{r}_N) dr_1 ... dr_N \tag{42}$$

The direct integrals may thus be reduced to three-dimensional quadrature.

Numerical quadrature is only used to evaluate bound-free and free-free matrix elements of the kinetic energy, nuclear attraction and direct transition potential operators. We require a set of points and weights in the space $\vec{r} = (x,y,z)$. The prerequisite for any quadrature is that we be able to construct the integrand at points in three-space. For example, for a bound-free potential matrix element, $\left\langle \varphi_k | V_{nuc} + V_{ij} | g^{\vec{r}'}_{\ell' m'} \right\rangle$, we need Gaussian basis functions which contribute to φ_k, a continuum function and a spherical harmonic evaluated at the points in $\vec{r}$-space, as well as the potential $V_{ij}(\vec{r})$. The Gaussian functions and nuclear attraction potential, V_{nuc}, are of course given by simple formulas, the spherical harmonic functions can be evaluated by efficient recursion schemes and the continuum functions by the procedures described earlier. For the moment, let us assume we also have a way to generate the potential $V_{ij}(\vec{r})$; we will return to this point momentarily. We now turn our attention to the construction of the points and weights of the grid.

Three-dimensional quadrature of the integrals typically required in molecular problems are difficult to converge because the integrands are dominated by cusps at the atomic nuclei. It is near these integrable singularities that we must use the greatest care to avoid quadrature errors. Some time ago[17], we developed an adaptive 3-D quadrature scheme to address this problem. In this scheme, we begin with a grid which is separable in spherical coordinates consisting of shells of points chosen from standard 1-D quadratures. This grid is adapted to the molecular problem by choosing a denser spacing of points in those subshells which contain the nuclei. The grid is then further refined by transforming the points under an analytic mapping which has the effect of rearranging those points in the vicinity of each nucleus so that they are drawn in closer to the nuclei. Since the mapping is analytic, the Jacobian of the transformation can be easily evaluated. This procedure has been used in most previous applications of the complex Kohn method.

More recently, we have implemented a multi-center numerical integration scheme originally proposed by Becke[18] and which is currently being used in applications of density functional theory[41]. The idea is to decompose a single molecular integral into a sum of one-center, atomic-like integrations. Specifically, we write a general integral corresponding to a molecule with N atomic centers

$$I = \int f(r) d^3r \tag{43}$$

as

$$I = \sum_{n=1}^{N} \int w_n(r) f(r) d^3 r$$
$$\equiv \sum_n I_n \tag{44}$$

where w_n is a *relative weight* function which has the property that it is unity in the vicinity of nucleus n and vanishes in a well-behaved fashion near any other nucleus. The normalization must be such that, for any r,

$$\sum_{n=1}^{N} w_n(r) = 1 \quad . \tag{45}$$

Since the function $w_n(r)F(r)$ is well behaved near any nucleus $i \neq n$, the integral I_n should be easy to converge by numerical quadrature in a spherical polar coordinate system about the center n. Even though the integral I is decomposed into N separate integrals, the total number of quadrature points should be far less than what would be required to converge the integral in any single-centered coordinate system.

The weighting function proposed by Becke is based on a partitioning of coordinate space into the so-called Voronoi polyhedra associated with each nucleus, the ith of which is simply the locus of points closer to nucleus i than to any other nucleus. The Voronoi polyhedra have a convenient analytical definition in terms of the coordinates

$$\mu_{ij} = \frac{r_i - r_j}{R_{ij}} \tag{46}$$

where r_i and r_j denote distances from the point r to nuclei i and j, respectively, and R_{ij} is the internuclear separation. If we define the step function

$$s(\mu_{ij}) = \begin{cases} 1, & -1 < \mu_{ij} \leq 0 \\ 0, & 0 < \mu_{ij} \leq 1 \end{cases} \tag{47}$$

then the Voronoi polyhedron associated with nucleus i is defined by the product:

$$P_i(r) = \prod_{j \neq i} s(\mu_{ij}(r)) \quad . \tag{48}$$

This product is unity if r lies within the polyhedron and vanishes outside the cell. Choosing

$$w_n(r) = \frac{P_n(r)}{\sum_i P_i(r)} \tag{49}$$

clearly satisfies the normalization condition of Eq. (45) and provides a function which vanishes near all nuclei $i \neq n$; unfortunately, it does not provide a suitable function for numerical integration because of the step discontinuities at $\mu_{ij}=0$. We can get a suitable function by retaining the definitions in Eq. (49), but replacing the step function $s(\mu_{ij})$ with an analytic function that passes continuously from one to zero as μ_{ij} passes through zero. Becke proposes the function

$$s(\mu) = \tfrac{1}{2}(1 - f_q(\mu)) \tag{50}$$

where

$$\begin{aligned} f_1(\mu) &= g(\mu) \\ f_2(\mu) &= g(g(\mu)) \\ f_3(\mu) &= g(g(g(\mu))) \, , \, , \, , \end{aligned} \tag{51}$$

and

$$g(\mu) = \tfrac{3}{2}\mu - \mu^3 \quad . \tag{52}$$

Successively sharper switching functions are generated as q increases. Like Becke, we have found that q=3 generates the best results.

In summary then, the procedure we use to evaluate continuum matrix elements is to first choose a set of quadrature points independently about each atom. Or course, we can make use of any local symmetry to reduce the number of points required. In a case like H_2O, for example, we would place points about only one hydrogen atom and double their associated weights. We then sum over all points, multiplying the integrand at each point by the product of its quadrature weight and the relative weight defined by Eq. (49). We have found that this quadrature scheme provides more accurate results with fewer that half the number of points required by our original scheme.

Before closing this section, we take up the question of how to evaluate the direct transition potential defined in Eq. (42). This potential can be written in terms of a one-electron density matrix (or transition density matrix if $\Gamma \neq \Gamma'$), $\rho^{\Gamma\Gamma'}$:

$$V_{\Gamma\Gamma'}(\mathbf{r}) = \sum_{kk'} \rho^{\Gamma\Gamma'}_{kk'} \int \frac{\varphi_k(\mathbf{r}') \quad \varphi_{k'}(\mathbf{r}') d^3\mathbf{r}'}{|\mathbf{r} - \mathbf{r}'|} \tag{53}$$

The density matrices are constructed with the target state vectors obtained from the pseudo-(N+1)-electron CI previously described, to assure consistency between the numerically and analytically obtained matrix elements. We will drop the $\Gamma\Gamma'$ notation below with the understanding that we are considering one such potential. The bound functions, φ_k, appearing in Eq. (53) are simply sums of Gaussians so the integrals appearing in this equation are identical to nuclear attraction integrals with a nucleus at the position $\bar{\mathbf{r}}$. These

integrals are one-electron integrals which appear in any quantum chemistry computer code. An algorithm can be constructed which computes these for the $\vec{r}$ points in the quadrature grid. Although this algorithm can easily be constructed to make use of vectoriztion on vector architecture supercomputers and provides an exact evaluation of the potential, it can become quite time consuming , especially for large molecules, since it can typically require the computation of millions of one-electron integrals.

Alternatively, we can opt for a numerical determination of the direct potential. We begin by decomposing the density with the local weight function defined above:

$$\begin{aligned}\rho(r) &\equiv \sum_{\alpha,\beta}\rho_{\alpha\beta}\varphi_\alpha(r)\varphi_\beta(r)=\sum_n w_n(r)\rho(r)\\ &\equiv \sum_n \rho_n(r)\end{aligned} \tag{54}$$

We next expand each component, ρ_n, of the density in spherical harmonics about its respective center:

$$\rho_n(r) \equiv \sum_{\ell,m} Y_{\ell m}(\hat{r}_n)\rho_n^{\ell m}(r_n) \tag{55}$$

where

$$\rho_n^{\ell m}(r) = \int d\hat{r} Y^*_{\ell m}(\hat{r})\rho_n(r) \tag{56}$$

We use the index n on the angular and radial variables in Eq. (55) to underscore the fact that these quantities are defined in the local coordinate system attached to atom n. By using the familiar expansion of $1/|r-r'|$ in spherical harmonics[42], the direct potential defined by Eq. (53) is expressed as

$$V(r)=\sum_n \sum_{\ell,m} \frac{4\pi}{2\ell+1} Y_{\ell m}(\hat{r}_n) f_n^{\ell m}(r_n) \tag{57}$$

with

$$f_n^{\ell m}(r) = \left[\frac{1}{r^{\ell+1}}\int_0^r r'^{\ell} + r^{\ell}\int_r^\infty \frac{1}{r'^{\ell+1}}\right]\rho_n^{\ell m}(r')r'^2 dr' \tag{58}$$

The essential point to note is that the decompostion of the density into atomic components via Eq. (54) leads to very rapid convergence of the spherical harmonic expansions. This is in marked contrast to a single-center expansion of the potential which, for an arbitrary polyatomic molecule, can be quite slowly convergent.

The radial components of the density, $\rho_n^{\ell m}(r)$, are obtained by an angular quadrature on a mesh of radial points and the functions $f_n^{\ell m}(r)$ are generated at the mesh points using,

for example, Simpson's rule integration. The spherical harmonics can be analytically evaluated in any coordinate system by recursion. Since the function $f_n^{\ell m}(r)$ is only computed on a mesh of radial points with respect to its own center, it must be *interpolated* to provide values at the radial points with respect to other centers. We have found that this procedure can provide substantial computational speed over analytic evaluation of the direct potentials. We have also found this approach to offer significant advantages over a technique described by Becke and Dickson based on numerical solution of Poisson's equation, which is simply the differential form of Eq. (53)[43].

Pseudoresonances and Intermediate Energy Scattering

The foregoing discussion, which has concentrated on the mechanics of how the variational equations are constructed and solved, shows that the complex Kohn formulation admits the use of multi-configuration target wave functions and large-scale optical potentials and that modern electronic structure techniques can be used to carry out most of the manipulations required quite efficiently. We now wish to turn our attention to the physical considerations of the underlying approximations that determine the partitioning of P-space and Q-space terms and the criteria we use for selecting the appropriate configurations to include in the trial wave function.

In applying the close-coupling formalism, we are confronted with two problems. The first problem is that, with the exception of single-electron atoms and ions, exact target states are not known and approximate wave functions must be used. These are generally expressed as linear combinations of CSF's built from a specified list of "target" orbitals. Moreover, since it is not practical to employ non-orthogonal functions in many-electron applications, we have imposed a strong orthogonality constraint between the scattering functions and the target orbitals[44-46]. It is well known that this constraint can lead to physically incorrect results if it is not relaxed, as was seen in early calculations on electron impact dissociation of H_2[47,48]. The standard remedy for removing this constraint, which is to include all (N+1)-electron penetration terms that arise by taking the direct product of the target orbitals and the various open-shell N-electron target configurations, can lead to an enormous number of terms as the expansion of the target wave functions is increased. In addition, anomolous pseudoresonances can arise at intermediate energies as a consequence of these terms[32].

Second, there is the obvious difficulty that, as the incident energy in a collision is increased toward the ionization energy, the number of open channels approaches infinity. Practical considerations thus generally limit the number of target states that can be included in a close-coupling calculation. Even if one is only interested in cross sections for excitation to low-lying excited states, these cross sections may be needed at energies well above the thresholds of other (bound and continuum) states. It is, therefore, natural to inquire about the effect of neglected channels at intermediate collision energies and to examine whether there is anything about the close-coupling formulation that might lead to pathological results. As we shall see, both of the difficulties just mentioned can lead to problems that are symptomatic of the same disease.

We can illustrate the kind of problem that may arise with the simple example of elastic scattering of an electron from H_2 in $^2\Sigma_g^+$ symmetry. If we use a simple configuration-interaction wave function of the form $(C_1\, 1\sigma_g^2 + C_2\, 1\sigma_u^2)$, with $C_1 >> C_2$, for the ground-state $X^1\Sigma_g^+$ wave function, the formalism we have outlined would dictate that we include a single penetration term $1\sigma_u^2\, 1\sigma_g$ in the trial wave function to relax the orthogonality constraint on the scattering wave function with respect to the $1\sigma_g$ orbital. The elastic cross section so calculated is shown in Fig. 1. There is evidently a broad resonance near 16 eV. Elastic scattering cross sections obtained with a simple self-consistent field (SCF) target wave function, which differs only slightly from the target CI wave function we used, show no such structure. Moreover, if the calculation is performed without the $1\sigma_u^2\, 1\sigma_g$ term, the resonance disappears. This result is also shown in Fig. 1.

The $1\sigma_u^2\, 1\sigma_g$ term can be thought of as a doubly excited negative ion term whose parent is the $(1\sigma_g\, 1\sigma_u)$, $b^3\Sigma_u^+$ state of H_2. This state is physically open at energies above 10 eV, but is not properly included in the single channel calculation. To demonstrate this, we performed a third calculation in which the $X^1\Sigma_g^+$ and $b\,^3\Sigma_u^+$ states were both included in the open channel portion of the trial function and the single penetration term was again retained. The resulting elastic cross section, shown in Fig. 1, is

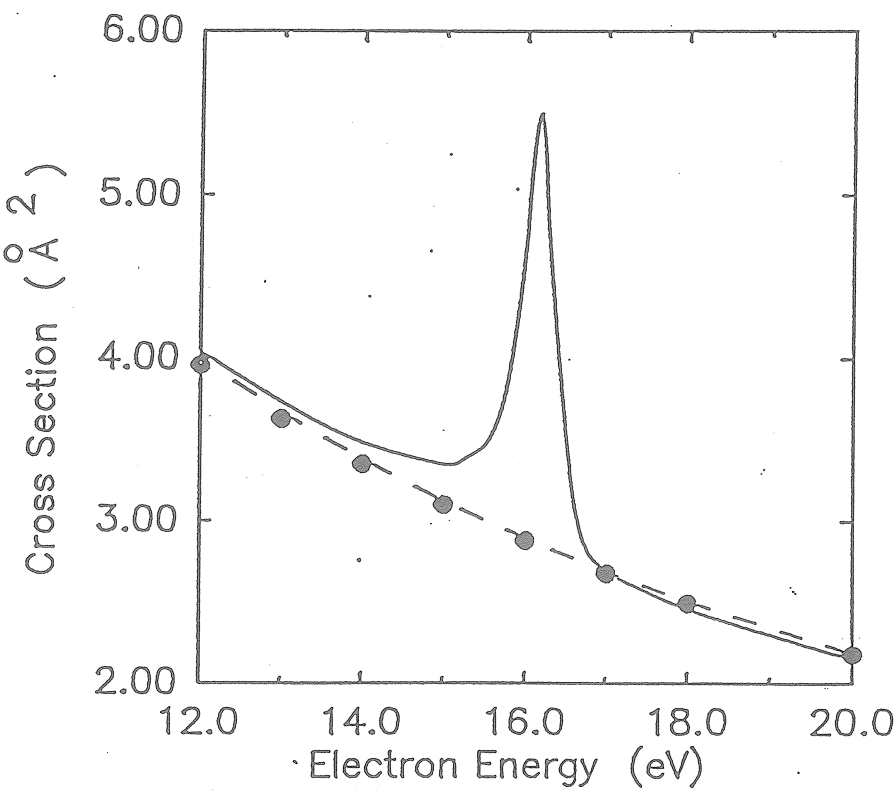

Figure 1. $e^- + H_2\ \Sigma_g^+$ elastic cross section. Solid curve: static-exchange plus penetration term; broken curve: static-exchange without penetration term; solid circles: 2-channel calculation including penetration term.

evidently quite close to the smooth result obtained from the single channel calculations in which the penetration term was dropped. This simple example serves to show how excited states, which are not explicitly included in the close-coupling expansion, can enter the problem in an indirect way when correlated target wave functions are used. In this simple case, it is possible to easily identify the cause of the trouble and remove the term responsible for this behavior from the single-channel trial function.

Another thing to note about the formalism as outlined above is that, in the case of multi-configuration target states, it provides more flexibility than the minimum needed to compensate for any orthogonality constraints, since the coefficients of the *individual* penetration terms are chosen variationally. However, all that is required to remove the target orthogonality constraints are the penetration terms that appear in fixed linear combinations that are consistent with the approximate target states that are being employed. We have shown elsewhere that it is possible to develop an algorithm for incorporating the penetration terms in these fixed linear combinations[32]. When elaborate CI target wave functions are used, this procedure can exclude many of the individual penetration terms built from N-electron configurations that contribute weakly to the target states explicitly chosen. Moreover, this contraction of the Hilbert space component of the total wave function makes it easier to identify and eliminate the terms in the trial wave function that will give rise to pseudo-resonances. To illustrate the power of this formalism, we show in Fig. 2 integral cross

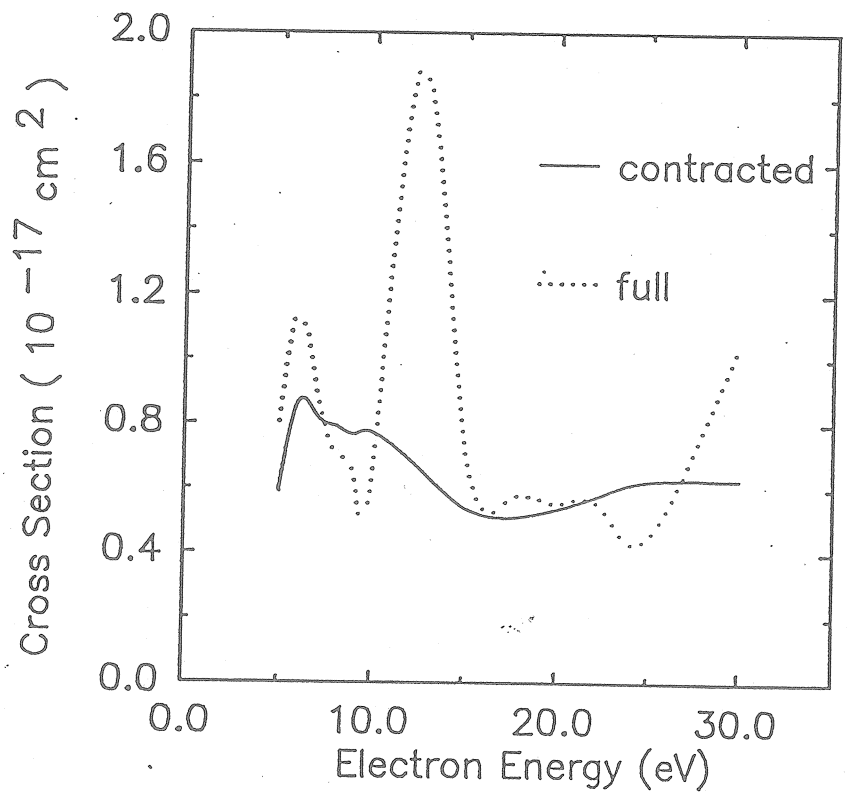

Figure 2. Total cross sections for $e^- + F_2, X^1\Sigma_g^+ \rightarrow 1^3\Pi_u$.

sections for electron impact excitation of the dissociative $1^3\Pi_u$ state of F_2[32]. The cross sections were obtained from three-state ($X^1\Sigma_g^+$, $1^3\Pi_u$, and $1^3\Pi_u$) close-coupling calculations using correlated target states and illustrate the unphysical pseudoresonances that occur as a result of including uncontracted penetration terms in the trial function. An approximate, but simpler, alternative to the procedure just outlined is to only include those penetration terms that arise from the dominant configuration for each target state[49-51]. Either of these techniques will allow one to meaningfully apply the close-coupling method at intermediate energies even when elaborate multi-reference target states are employed.

A note about the target orbitals bears further comment. The previous discussion has presupposed the existence on an orbital set in terms of which the target wave functions have a compact representation so that it is easy to identify a principal configuration for each target state. For this reason, we have emphasized the use of averaged natural orbital techniques in many of our studies[30,32,49-52], since this often provides an ideal way to achieve a compact representation for a number of excited states without overly compromising on the accuracy.

APPLICATIONS AND EXTENSIONS

Off-Shell Extension to Threshold Vibrational Excitation

Much of the theoretical literature on electron-molecule scattering has focused on the development of *ab initio* methods for solving the electronic fixed-nuclei problem; this review is no exception. The complex Kohn technique, like other sophisticated methods presently available for tackling the low-energy electron-molecule scattering problem, has been implemented within the framework of the adiabatic-nuclei approximation[53]. In many cases, meaningful cross sections can be extracted solely from fixed-nuclei calculations, while in other cases the fixed-nuclei electronic problem can provide the input necessary to solve the full problem including the nuclear dynamics[22]. However, there are many interesting cases where the adiabatic-nuclei approximation breaks down.

The assumption that underlies the adiabatic-nuclei approximation is that the target molecule is effectively fixed during the course of the collision; this approximation consequently provides an accurate description of electron-molecule scattering only when the collision time is short compared with the rotational and vibrational periods of the molecule. This assumption of course breaks down in near-threshold regions where cross sections computed with the adiabatic-nuclei approximation do not vanish at the appropriate thresholds[54]. The breakdown of the adiabatic-nuclei approximation can be particularly severe for light molecules with large vibrational energy spacings (eg. ~.5 eV in H_2).

Laboratory-frame close-coupling, in which the total wave function is expanded in terms of the rotational, vibrational and electronic states of the target along with angular momentum states of the projectile[55], provides the most rigorous approach to electron-molecule collisions. Unfortunately, it becomes unwieldy for all but the simplest targets and, to date, has proved to be impossible for systems other that $e^- + H_2$. Body-frame

vibrational close-coupling[56], in which only the rotational motion is treated adiabatically, is somewhat easier to apply; however, even this approach has relied on model potentials for all or part of the electron-target interaction and has yet to be carried out in a completely *ab initio* context.

In 1975, Shugard and Hazi[57], in a paper that examined the underpinnings of the adiabatic-nuclei approximation, suggested that an off-the-energy-shell generalization of the T-matrix (scattering amplitude) could extend the range of validity of the adiabatic-nuclei approximation while retaining much of its inherent simplicity. Their basic idea was to employ the approximate expressions for scattering amplitudes given by the adiabatic-nuclei approximation, but to use the proper energies in the entrance and exit channels. A numerical verification of soundness of these early ideas was provided some years later by Morrison and coworkers[58] in calculations of $e^- + H_2$ vibrational excitation carried out with model potentials. The off-shell treatment, which they termed the first-order nondegenerate adiabatic (FONDA) approximation, gave cross sections that were far more accurate than those given by conventional adiabatic-nuclei theory, and almost identical to those obtained from a full close-coupling treatment.

The complex Kohn method can be modified to provide a computational tool for variational evaluation of the off-shell T-matrix in a completely general *ab initio* context. We begin by noting that the T-matrix, whose elements we have defined by the asymptotic behavior of a trial wave function, also has a formal definition[59] as the matrix element

$$T^{el}{}_{i\to f} = \langle \Psi'_o | V | \Psi^+ \rangle \tag{59}$$

where Ψ^+ is the full scattering wave function for the N+1 electron system, Ψ'_o is the corresponding unperturbed wave function and V is that part of the full Hamiltonian that describes the electron-target interaction. We wish to evaluate this quantity "off the energy shell" and so the prime on Ψ'_o indicates that it is not evaluated at the same total energy as is Ψ^+.

Ψ^+ is of course antisymmetric under interchange of any pair of electron coordinates, but Ψ'_o is not and V is not a symmetric operator. Hence, Eq. (59) is not a convenient expression for many-body applications. We can of course also write the T-matrix as

$$T^{el}{}_{i\to f} = \langle \Psi^- | H - E' | \Psi'_o \rangle \tag{60}$$

since

$$(H_o - E')\Psi'_o = 0 \tag{61}$$

where H_0 is the unperturbed Hamiltonian and $H = H_0 + V$. Since $H - E'$ is a symmetric operator, we can now antisymmetrize Ψ'_o in Eq. (60) without changing the resulting value of $T^{el}{}_{i\to f}$.

It is possible to develop a variational principle for $T^{el}{}_{i\to f}$ by following the procedure given by Gerjouy, Rau and Spruch[60]. Defining $W \equiv (H - E')\Psi'_o$, a stationary principle for $T^{el}{}_{i\to f}$ is given by:

$$T^{s}{}_{i\to f} = \langle \Psi^{-t} | W \rangle + \langle f^t | H - E | \Psi^{+t} \rangle \tag{62}$$

where the auxiliary trial function f^t satisfies the equation

$$(H - E)|f^t\rangle + |W\rangle = 0 \tag{63}$$

along with the boundary condition

$$\langle f^t | H - E | \delta\Psi^{+t} \rangle - \langle \delta\Psi^{-t} | H - E | f^t \rangle = 0 \tag{64}$$

where

$$\delta\Psi^{\pm t} = \Psi^{\pm t} - \Psi^{\pm}. \tag{65}$$

We now choose a trial scattering wave function of the same form given in Eqs. (25-26) but, for notational simplicity, we assume there is only one electronically open channel:

$$\Psi^{+} = A(\chi\, F_{\Gamma_0}) + \sum_{\mu} d_{\mu}^{\Gamma_0} \Theta_{\mu} \quad , \tag{66}$$

with

$$F_{\Gamma_0} = \sum_i c_i\, \varphi_i + \sum_{\ell m} [f_{\ell m}(k\, r)\delta_{\ell\ell_0}\delta_{mm_0} + T^{t}_{\ell\ell_0 mm_0} g_{\ell m}(k_\Gamma r)] \tag{67}$$

where the $T^{t}_{\ell\ell_0 mm_0}$ are now to be regarded simply as a set of trial parameters. The boundary condition specified by Eq. (64) is satisfied by expanding f^t as[61]

$$f^t = \sum_i a_i\, \varphi_i + \sum_{\ell m} [b_{\ell\ell_0 mm_0} g_{\ell m}(k_\Gamma r)] \tag{68}$$

The derivation proceeds along the same lines we outlined in our earlier discussion of potential scattering; by carrying out the variation with respect to the linear coefficients in Eqs. (66) and (67), we get a stationary expression for the off-shell T-matrix elements:

$$T^{s}_{\ell\ell_0 m m_0} = \langle A\chi f_{\ell m} | H - E' | A\chi j'_{\ell_0 m_0} \rangle - \sum_{\alpha,\beta} \langle A\chi f_{\ell m} | H - E | \alpha \rangle \langle \alpha | H - E | \beta \rangle^{-1} \langle \beta | H - E' | A\chi j'_{\ell_0 m_0} \rangle \tag{69}$$

where α and β refer to the space spanned by the functions $A\chi\varphi_i$ and $A\chi g_{\ell m}$. We have again adopted the convention of using g_{lm} to denote the product of a radial function and Y_{lm}/r. Note that the term $j'_{\ell_0 m_0}$ on the RHS of Eq. (69) arises from the partial wave expansion of the plane-wave part of the unperturbed wave function Ψ'_0.

The variational expression for the off-shell T-matrix, Eq. (69), is clearly similar to the result we developed for the more familiar on-shell result, Eq. (30), but there are some key differences to note. Aside from the obvious fact that the continuum functions f_ℓ (and g_ℓ) are evaluated at a momentum that differs from the value used in j'_ℓ, there is a more subtle difference. The on-shell T-matrix has the property of *transfer invariance* [11], which means that it is not changed by any transformation which mixes an arbitrary component of the square-integrable functions φ_i into the continuum functions. Thus, in the on-shell case, the function j_ℓ could be replaced by f_ℓ without changing the result (recall that we constructed f_ℓ to be orthogonal to all the square-integrable basis functions). In the on-shell case, we used this fact to eliminate an entire class of bound-free and free-free exchange matrix elements[16] by using separable approximations of the form:

$$H^{ex} \approx \sum_{i,j} |i\rangle\langle i| H^{ex} |j\rangle\langle j| \quad . \tag{70}$$

The off-shell T-matrix, by contrast, is only transfer invariant with respect to the functions f_ℓ and g_ℓ, which appear in the expansion of the trial wave function Ψ^{+t}, but not the functions j_ℓ. The latter cannot be arbitrarily orthogonalized to the functions φ_i. Thus, continuum matrix elements involving j_ℓ can be simplified by using separable expansions, but not eliminated entirely.

To compute an amplitude for vibrational (or rotational) excitation, we evaluate the off-shell T-matrix for different nuclear geometries and use the adiabatic approximation [62]:

$$T(k_0 \rightarrow k_f) = \int dR\, v_0(R)\, T^{el}_{0\rightarrow f}(R)\, v_f(R) \tag{71}$$

where v_0 and v_f are the initial and final nuclear target wave functions and R denotes the appropriate nuclear coordinates. The wave vectors k_0 and k_f are simply chosen to conserve the total energy in the initial and final channels. Thus, aside from the use of an off-shell electronic T-matrix, the procedures for computing excitation cross sections are identical to those used in the adiabatic-nuclei approximation.

We carried out an *ab initio* treatment of low-energy $e^- + H_2$ scattering[63], using the off-shell formalism just described, in an effort to help resolve a longstanding dilemma posed by the discrepancy between crossed-beam measurements of the vibrational excitation cross section of H_2[64] and valued derived from an analysis of swarm data[65]. Previous theoretical

treatments of this problem were based on a Hartree-Fock wave function for the target H_2 molecule and correlation effects were modelled with a local potential[66]. Because the vibrational excitation cross section is sensitive to the R-dependence of the electronic amplitudes, as well as to the dynamic distortion of the target molecule, we used a two-term $\left(c_1 1\sigma_g^2 + c_2 1\sigma_u^2\right)$ target wave function with natural orbitals extracted from a configuration-interaction expansion. The dynamic distortion of the target was treated by including in the Kohn trial function energetically closed electronic channels in the form of direct products of a bound orbital and a two-electron state formed by singly exciting the ground state target wave function into a large set of virtual orbitals.

Fig. 3 compares our calculated result for the integrated vibrational excitation cross section with previous theory[66] as well as available experimental data[64,65,67,68]. Our results are clearly in better agreement with the crossed-beam data than with the swarm derived cross sections. The agreement with the most recent experiments of Brunger et al.[64] is particularly good. There is also excellent agreement between our result and the theoretical results of Buckman et al.[66] (which used a model polarization potential in a full body-frame vibrational close coupling treatment) in the energy range below 1.6 eV, although our calculated cross section is somewhat smaller at higher energies. It is noteworthy that when we carried out our calculations with an uncorrelated target wave function, we obtain a result which is closer to that of Buckman et al. , which also used an SCF target wave function.

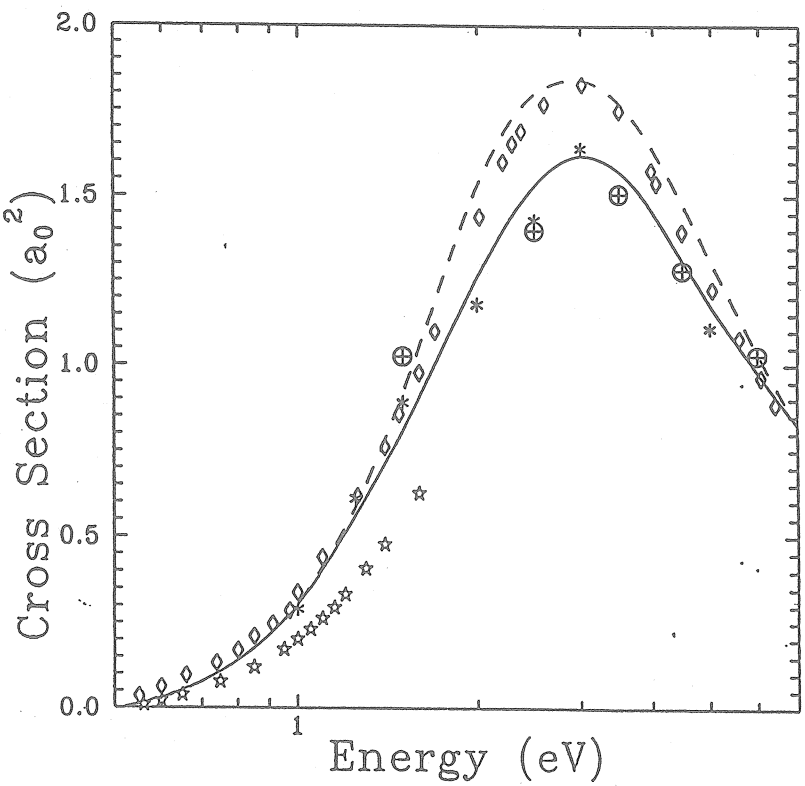

Figure 3. Integral cross sections for 0→1 vibrational excitation. Solid curve, off-shell Kohn result (ref. 63); dashed curve, theoretical result of Buckman et al. (re. 66); asterisks, Brunger et al. (ref. 64); circles, Linder and Schmidt (ref.67); diamonds, Ehrhardt et al. (ref. 68); stars, swarm results (ref. 65).

The vibrational excitation cross section is dominated by a broad, negative ion shape resonance of $^2\Sigma_u^+$ symmetry which shows a strong dependence on internuclear separation. The $^2\Sigma_u^+$ shape resonance is evidently softened when a correlated target function is employed, resulting in a smaller cross section. Our calculations, coupled with previous theoretical work, strongly support the validity of the crossed-beam measurements of vibrational excitation in H_2.

In cases where the threshold vibrational excitation cross section displays no anomolous behavior, the off-shell T-matrix formalism, which correctly conserves energy in the entrance and exit channels, provides a simple way of extending the validity of conventional adiabatic-nuclei theory. There are other cases, however, where vibrational excitation cross sections display prominent threshold features that cannot be explained on the basis of simple threshold laws[54]. Such is the case with the hydrogen halides[69], where the sharp threshold peaks that have been the subject of much theoretical study over the years[54] evidently correspond to nuclear-excited Feshbach resonances whose proper description requires more than a simple modification of adiabatic-nuclei theory[70]. It is interesting to question whether the simple off-shell theory is ever applicable in situations where threshold features are present. The CH_4 molecule provides an interesting example since it possesses no permanent dipole moment, but nevertheless displays vibrational excitation cross sections that rise steeply from threshold[71,72]. We have recently found that the present formalism can provide a qualitatively accurate description of the observed effects[73].

The first thing to note about e^-+CH_4 is that the *elastic* cross section shows a pronounced Ramsauer-Townsend minimum near .4 eV[74], a fact which, coupled with the absence of a stable negative ion, is consistent with the presence of a virtual state[54]. Accurate *ab initio* calculations carried out at the equilibrium geometry have reproduced the observed elastic cross section in the energy region of the Ramsauer-Townsend minimum[31]. One might expect the position of this minimum to be sensitive to nuclear geometry, in which case the off-shell T-matrix formalism, which is guaranteed to give a vibrational excitation cross section that vanishes at threshold, could give a qualitatively correct description of the observed results.

We have carried out complex Kohn calculations on this system at selected geometries using the off-shell formalism previously outlined. The methane molecule has nine normal modes of which, due to symmetry considerations, only four are energetically different. We studied the non-degenerate, Raman-active ν_1(symmetric stretch) and triply-degenerate, infrared-active ν_3 modes, which have threshold energies of 362 and 374 meV, respectively. The electron-energy-loss peaks corresponding to these transitions are not resolved in current experiments. The trial wave functions were constructed along the same lines that we found to be successful in our earlier studies of elastic scattering[31]. We used an SCF description of the ground-state target wave function and included single excitations of the target into a compact space of polarized orbitals.

For the symmetric stretch mode, the "fixed-nuclei" elastic cross sections computed from the off-shell amplitudes are plotted in Fig. 4 at five different values of the C-H bond

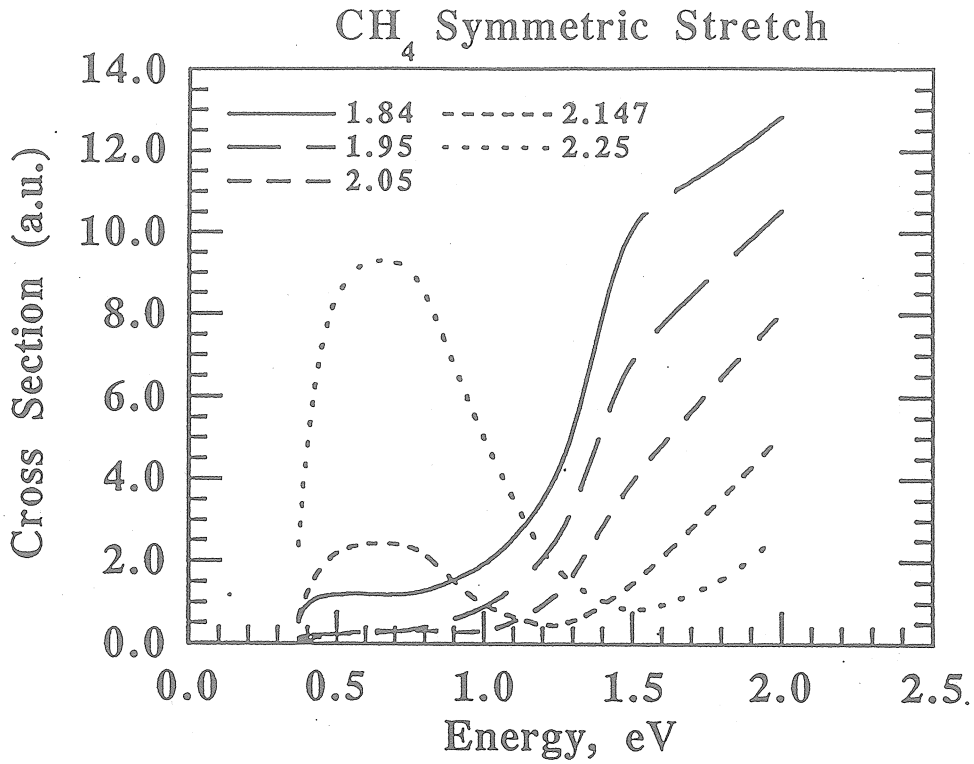

Figure 4. Fixed-nuclei elastic cross sections computed from the off-shell T-matrix for different C-H bond lengths along the symmetric stretch mode. The equilibrium CH distance in 2.05 Bohr.

length. These cross sections rise from the 362 meV threshold with vertical onset that is characteristic of an s-wave inelastic process. For the larger C-H bond values, the cross sections rise to a prominent peak before decreasing through a Ramsauer-Townsend minimum. This behavior is less pronounced for the shorter C-H values since the RT minimum moves below the vibrational threshold energy as the CH bond is squeezed below its equilibrium value. We also carried out variational calculations for several values of the normal coordinate corresponding to one of the three degenerate infrared-active ν_3 modes.

Fig. 5 shows both the ν_1 and ν_3 contributions to the total vibrational excitation cross section, which were obtained by using off-shell amplitudes in Eq. (71) along with harmonic oscillator functions for the vibrational wave functions. It is interesting to note that the minimum at 1.25 eV, which reflects the geometry dependence of the fixed-nuclei Ramsauer-Townsend minimum, is less pronounced in the ν_3 cross section. This is to be expected, since the RT minimum is basically an s-wave phenomenon. The ν_3 mode, however, is infrared-active, which means that there is a transition dipole associated with motion in this mode. There is consequently a coupling between s-waves and p-waves that occurs in this mode which is not present in the symmetric-stretch amplitude. This coupling tends to wash out the effect of the RT minimum.

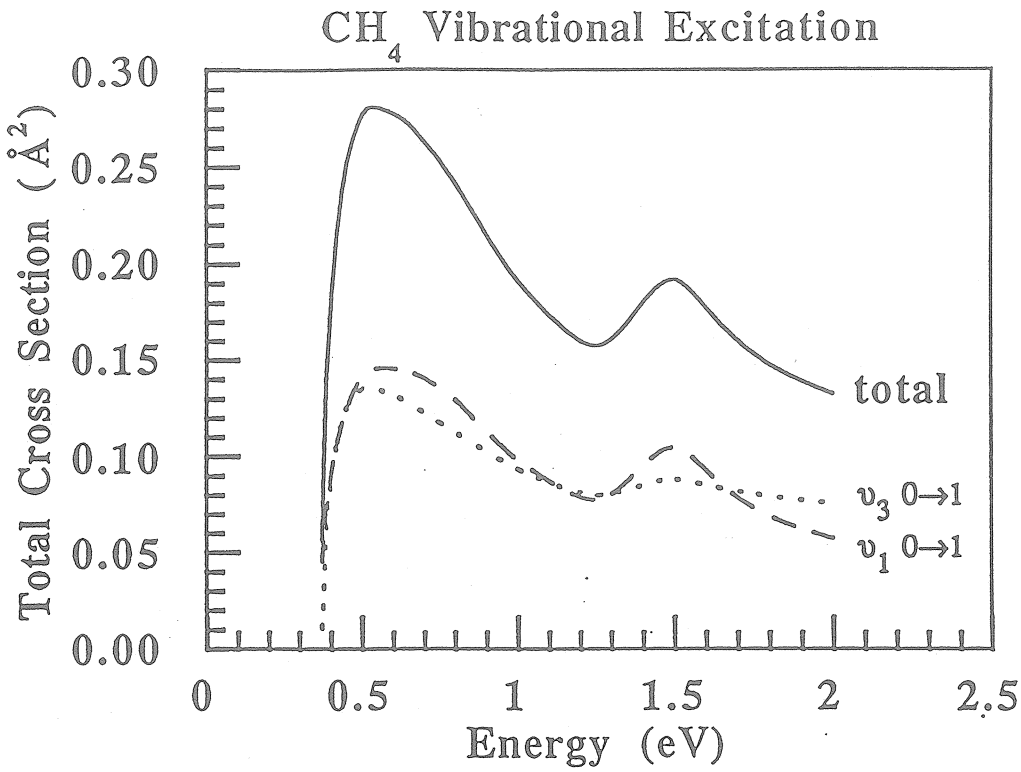

Figure 5. Electron-CH_4 vibrational excitation cross sections for the ν_1 and ν_3 normal modes.

Polar molecules

There are several complications one encounters when studying electron scattering by polar molecules. Because of the long-range character of the underlying electron-dipole interaction, which behaves asymptotically as $\mathbf{D}\cdot\mathbf{r}/r^3$, where $\mathbf{D}$ is the permanent dipole moment of the target, it turns out that many partial-wave components are needed to properly describe scattering for small deflection angles of the incident electron and to obtain converged total cross sections. One also has the additional *formal* difficulty that a fixed-nuclei treatment of electron scattering by a polar molecule gives infinite total cross sections and differential cross sections that diverge at zero scattering angle, which is a consequence of ignoring the rotational motion of the target molecule[75,76]. We will show that the solution to *both* problems is to exploit the fact that beyond a certain ℓ cutoff the partial-wave components of the scattering functions do not penetrate the interior part of the molecular target. This allows us to use a hybrid treatment in which only the low order partial-wave components of the T-matrix are determined from variational calculations and the higher order terms are included in the Born approximation via a closure formula. In the course of this discussion, we will also describe the numerical techniques we use to calculate differential cross sections, which differ from the procedures commonly used.

Let us first consider the case of a *non-polar* target. When the incident electron energy is large compared to the rotational energy spacings of the molecule, one is usually justified in

ignoring the rotational motion of the target and treating the scattering as that produced by an ensemble of randomly oriented, motionless targets[77]. Under this assumption, the differential cross section for exciting a molecule from initial electronic state Γ and vibrational state v to final states Γ', v' can be expressed as:

$$\frac{d\sigma}{d\omega}(\Gamma v \rightarrow \Gamma' v') = \frac{(4\pi)^2}{k_\Gamma^2} \int \frac{d\alpha \, d\cos\beta d\gamma}{8\pi^2} |\langle k_{\Gamma'} v' | T^{\Gamma\Gamma'} | k_\Gamma v \rangle|^2 \tag{72}$$

where α, β and γ are the three Euler angles that orient the initial and final wave vectors k_Γ and $k_{\Gamma'}$ with respect to the target. The laboratory scattering angle ω is the angle between k_Γ and $k_{\Gamma'}$. The body-frame T-matrix has the expansion:

$$\langle k_{\Gamma'} v' | T^{\Gamma\Gamma'} | k_\Gamma v \rangle = \sum_{\substack{\ell\ell' \\ mm'}} i^{\ell-\ell'} Y_{\ell m}(k_\Gamma) \, Y^*_{\ell' m'}(k_{\Gamma'})$$
$$\times \int \chi_v(s) T^{\Gamma\Gamma'}_{\ell m \ell' m'}(s) \chi_{v'}(s) ds \tag{73}$$

where we have used s to denote the internal vibrational coordinates of the target and the vibrational wave functions are χ_v and $\chi_{v'}$. If we are not interested in the individual vibrational levels and simply wish total cross sections associated with a particular electronic transition, we can sum Eq. (72) over the final vibrational levels of the target. If we assume that the electron kinetic energy is large compared to the spacing between vibrational levels, then we can use closure,

$$\sum_{v'} \chi_{v'}(s) \chi_{v'}(s') = \delta(s - s') \tag{74}$$

to obtain

$$\frac{d\sigma}{d\omega}(\Gamma \rightarrow \Gamma')_{\text{total}} = \int \chi_v(s) \frac{d\sigma^{\Gamma\Gamma'}}{d\omega}(s) \chi_v(s) ds \tag{75}$$

Thus, the vibrationally summed cross section is expressed as the expectation value of the fixed-nuclei cross section with respect to the initial vibrational state of the target. One frequently approximates this quantity by the value of the fixed-nuclei cross section obtained at the equilibrium geometry of the target.

The usual procedure for carrying out the angular average required in Eq. (72) is to use Wigner rotation matrices to express the spherical harmonics that appear in Eq. (73) in laboratory frame coordinates and then carry out the averaging analytically[77]. Alternatively, we can carry out the integrations in Eq. (72) by numerical quadrature, keeping the angle between k_Γ and $k_{\Gamma'}$ fixed. Starting with an initial pair of wave vectors k_{Γ_o} and $k_{\Gamma'_o}$ in the body frame, we can express the wave vectors needed to evaluate the integrand for any set of Euler angles, from the expression[78]:

$$k_\Gamma(\alpha,\beta,\gamma) = \begin{bmatrix} \cos(\alpha)\cos(\beta)\cos(\gamma)-\sin(\alpha)\sin(\gamma) & -\cos(\alpha)\cos(\beta)\sin(\gamma)-\sin(\alpha)\cos(\gamma) & \cos(\alpha)\sin(\beta) \\ \sin(\alpha)\cos(\beta)\cos(\gamma)+\cos(\alpha)\sin(\gamma) & -\sin(\alpha)\cos(\beta)\sin(\gamma)+\cos(\alpha)\cos(\gamma) & \sin(\alpha)\sin(\beta) \\ -\sin(\beta)\cos(\gamma) & \sin(\beta)\sin(\gamma) & \cos(\beta) \end{bmatrix} k_{\Gamma 0} \tag{76}$$

This numerical approach allows us to avoid the complex angular momentum algebra necessitated by an analytic formulation and substantially reduces the complexity of the coding required. It also makes it fairly easy to carry out the modifications of the fixed-nuclei approach that are necessary in order to study electron collisions with *polar* molecules.

For elastic scattering by polar targets, a useful strategy is to expand the *difference* between the desired T-matrix and its value in the first Born approximation as a rapidly convergent partial-wave series and then to use a completion formula to obtain the final result. (Note that similar considerations apply to the case of inelastic, dipole-allowed allowed transitions.) The partial-wave Born approximation for the *electronically* elastic ($\Gamma \rightarrow \Gamma$) T-matrix element is given by

$$_{B}T^{\Gamma\Gamma}_{\ell m \ell' m'} = 2\sqrt{k_\Gamma k_\Gamma} \int j_{\ell'}(k_{\Gamma'} r)\, Y^*_{\ell' m'}(\hat{r})\, (\chi_\Gamma H \chi_\Gamma)\, j_\ell(k_\Gamma r)\, Y_{\ell m}(\hat{r})\, d^3r \tag{77}$$

Consistent with this approximation is the replacement of $(\chi_\Gamma H \chi_\Gamma)$ by its asymptotic form[79]:

$$\begin{aligned} V_{\Gamma\Gamma}(r) &= (\chi_\Gamma\, H \chi_\Gamma) \\ &\equiv \int \chi_\Gamma(r_1,,r_N)\, H(r,r_1,,r_N)\, \chi_{\Gamma'}(r_1,,r_N) \\ &\sim D\cdot \hat{r}/r^2 \end{aligned} \tag{78}$$

where D is the dipole moment and $\hat{r}$ is a unit vector in the body frame of the molecule. With this limiting form of the potential, the first Born approximation gives extremely simple formulas for scattering amplitudes and cross sections that can serve as a useful starting point for a more elaborate treatment of the dynamics. For example, the full body-frame, fixed-nuclei T-matrix is given as[75]:

$$\begin{aligned} \langle k_{\Gamma'} | {}_{B}T^{\Gamma\Gamma} | k_\Gamma \rangle &= -\frac{\sqrt{k_\Gamma k_{\Gamma'}}}{8\pi^2} \int e^{-i(k_\Gamma - k_{\Gamma'})\cdot r} \frac{D\cdot \hat{r}}{r^2}\, d^3r \\ &= -\frac{\sqrt{k_\Gamma k_{\Gamma'}}\; i\, D\cdot \widehat{k'}}{2\pi\, |k_\Gamma - k_{\Gamma'}|} \end{aligned} \tag{79}$$

where $\widehat{k'} = (k_{\Gamma'} - k_\Gamma)/|k_{\Gamma'} - k_\Gamma|$. We now write the partial wave expansion of the exact body frame T-matrix in the following form:

$$\left\langle k_\Gamma \middle| T^{\Gamma\Gamma} \middle| k_{\Gamma'} \right\rangle = -\frac{\sqrt{k_\Gamma k_{\Gamma'}}\, i\, \mathbf{D}\cdot\hat{\mathbf{k}}'}{2\pi^2 \left| k_\Gamma - k_{\Gamma'} \right|}$$

$$+ \sum_{\substack{\ell'\ell \\ mm'}} i^{\ell-\ell'} Y^*_{\ell' m'}\left(\hat{k}_{\Gamma'}\right) Y_{\ell m}\left(\hat{k}_\Gamma\right)\left(T^{\Gamma\Gamma}_{\ell m \ell' m'} - B T^{\Gamma\Gamma}_{\ell m \ell' m'}\right) \tag{80}$$

where we have merely added and subtracted the Born approximation to the partial wave expansion of the exact T-matrix. The point to note is that the sum in Eq. (80) now contains differences between exact and Born partial wave elements, which rapidly approach zero as $\ell(\ell')$ get large. To obtain converged cross sections, we need only compute variational T-matrix elements to high enough ℓ where the Born approximation is accurate. To obtain differential cross sections (away from zero scattering angle) corresponding to a random orientation of the target molecule with respect to an incident electron beam in the laboratory frame, we simply substitute the amplitude defined in Eq. (80) into Eq. (72) and carry out the average over molecular orientations numerically.

In the usual fixed-nuclei approximation, which does not treat the motion of the nuclei dynamically, the magnitudes of k_Γ and $k_{\Gamma'}$ are identical and hence the Born amplitude in Eq. (80) diverges as the scattering angle approaches zero. Eq. (80) is nevertheless perfectly adequate for studying scattering out of the forward direction and for calculating momentum transfer cross sections, which are insensitive to the form of the differential cross section near zero degrees, as long as the electron energy is large compared to the spacing of the rotational levels[80].

To compute total cross sections for polar molecules, we must introduce the rotational motion of the target. However, as Padial and Norcross[81] have pointed out, this does not mean we have to carry out fully coupled laboratory frame calculations, which are slowly convergent and hence only feasible when model potentials are used. We can still use our hybrid formula, but following the suggestion of Padial and Norcross, we use *fixed-nuclei* quantities for the rapidly converging differences between partial-wave T-matrix elements and include rotational quantum numbers in the full Born amplitude, which removes the divergence in the forward direction. This is justified because, as Collins and Norcross[80] have demonstrated, for low angular momentum quantum numbers, the differences in the T-matrix elements obtained from lab-frame calculations and frame-transformed fixed-nuclei calculations are insignificant for polar targets.

We have carried out complex Kohn studies of elastic electron scattering by several polar molecules, including H_2O[82], NH_3[83] and, more recently, H_2S[84]. It is not surprising to find that at very low energies, where the cross sections are large, the results are largely determined by dipole Born approximation, while at high energies, the static-exchange approximation is adequate. In the energy range from 1-4 eV, however, polarization is found to be important. Fig. 6 shows results we obtained for H_2S, along with the experimental results of Gulley et al.[85]. The cross sections develop a significant backward peak as the energy increases, indicating a significant deviation from the Born approximation. This

backward peaking, which we found in all the polar systems we studied, is not evident from experimental measurements, which rarely extend beyond 120°. It is noteworthy that this large angle region contribites significantly to the determination of the momentum transfer cross section and that extrapolation of measured cross sections to large angles can be dangerous.

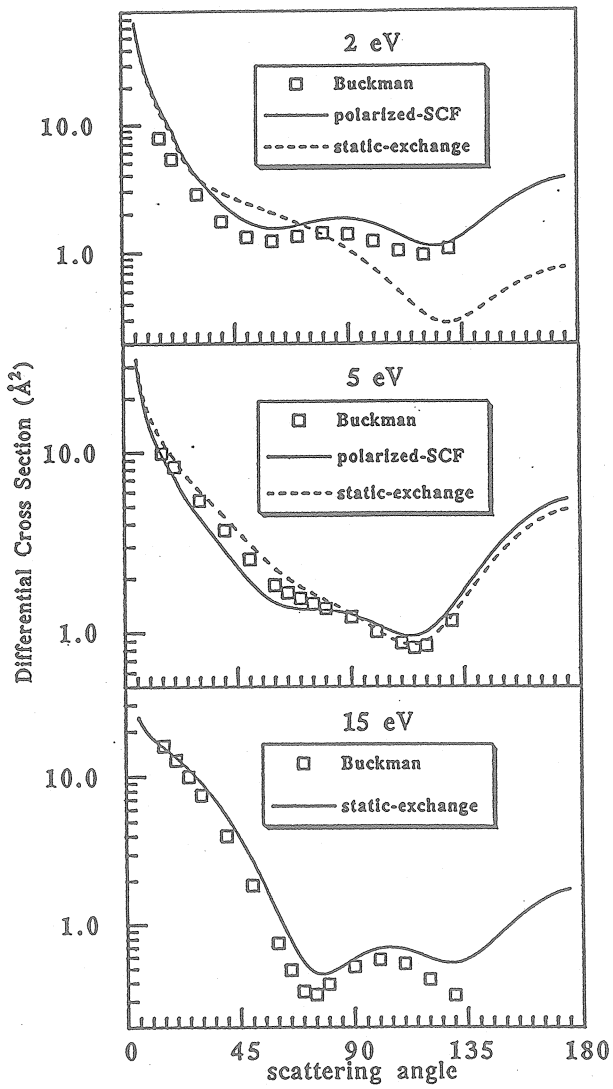

Figure 6. Differential cross sections for $e^- + H_2S$. Experimental points from ref. (85).

Photoionization

The complex Kohn method can be easily adapted to study molecular photoionization. We use a trial function of the same form as that given in Eq. (25), with incoming wave boundary conditions appropriate for scattering by an ionic target. The only difference

between the photionization case and scattering from a molecular ion is the normalization of the contiuum basis function. This is chosen such that

$$h_\ell^- (kr) \underset{r\to\infty}{=} \frac{1}{\sqrt{k}} e^{-i(kr-\ell\pi/2+\ln(kr)/k+\delta_\ell)} \tag{81}$$

where δ_ℓ is the Coulomb phase shift, yielding purely incoming, rather than outgoing waves.

The matrix elements needed to construct photoionization sections can be expressed in terms of the body-frame amplitudes[86]:

$$\begin{aligned} I^\mu_{\Gamma_o} &\equiv \langle \Psi_o | \mu | \Psi^-_{\Gamma_o} \rangle \\ &= \sum_{i=1}^{N} \int \Psi_o(r_1,,r_N) r_i^\mu \Psi^-_{\Gamma_o}(r_1,,r_N) d^3r_1..d^3r_N \end{aligned} \tag{82}$$

where r^μ is the dipole operator which, in the length form, is defined as

$$r^\mu = \begin{cases} z & ,\mu = 0 \\ \mp(x \pm iy)/\sqrt{2} & ,\mu = \pm 1 \end{cases} \tag{83}$$

and Ψ_0 is the wave function for the initial state of the target molecule. In order to construct an amplitude that represents an ejected photoelectron with momentum $\vec{k}_{\Gamma_o}$ associated with a particular ion channel, the matrix elements defined in Eq. (82) must be combined in a partial wave series

$$I_{\vec{k}_{\Gamma_o},\hat{\varepsilon}} = \sqrt{\frac{4\pi}{3}} \sum_{\ell_o m_o \mu} i^{\ell_o} e^{-i\delta_{\ell_o}} I^\mu_{\Gamma_o} Y^*_{1\mu}(\hat{\varepsilon}) Y^*_{\ell_o m_o}(\hat{k}_{\Gamma_o}) \tag{84}$$

where $\hat{k}_{\Gamma_o}$ specifies the direction of the ejected electron and $\hat{\varepsilon}$ is the direction of polarization of light. The doubly differential cross section for a hypothetical space-fixed target molecule is then given as

$$\frac{d^2\sigma^{\Gamma_o}}{d\Omega_{\hat{k}} d\Omega_{\hat{\varepsilon}}} = \frac{8\pi\omega}{3c} \left| I_{\vec{k}_{\Gamma_o},\hat{\varepsilon}} \right|^2 \tag{85}$$

where ω is the photon energy and c is the speed of light. In order to compute a cross section defined in the typical experiment where the target orientation is not resolved, the quantity defined in Eq. (85) must be averaged over all orientations of the target molecule in the laboratory frame. The resulting differential cross section has the form[87]

$$\frac{d\sigma^{\Gamma_o}}{d\Omega} = \left\langle \frac{d^2\sigma^{\Gamma_o}}{d\Omega_{\hat{k}} d\Omega_{\hat{\varepsilon}}} \right\rangle_{av} = \frac{\sigma^{\Gamma_o}}{4\pi}\left[1 + \beta^{\Gamma_o} P_2(\cos\theta)\right] \tag{86}$$

where P_2 is the Legendre polynomial of order 2, θ is the angle between $\hat{\varepsilon}$ and $\hat{k}$ and β^{Γ_o} is the so-called asymmetry parameter. We find it convenient to carry out the average required in Eq. (86) numerically, by a procedure analogous to the one we use to compute differential electron-molecule scattering cross sections. The quantity σ^{Γ_o} is the total photoionization cross section averaged over all polarizations and photoelectron directions and is given by

$$\sigma^{\Gamma_o} = \frac{8\pi\omega}{3c} \sum_{\ell_o m_o \mu} \left| I^{\mu}_{\Gamma_o} \right|^2 \tag{87}$$

We now turn our attention to the computation of the body-fixed amplitudes $I^{\mu}_{\Gamma_o}$. We choose a single set of molecular orbitals, $\{\varphi_i\}$, and partition them, as before, into a target set, in terms of which the initial state Ψ_0 and the ion states χ_Γ are expanded, and a complementary set of scattering orbitals for expanding the short-range part of the channel functions $F^{-}_{\Gamma_o\Gamma}$. It is clear that the amplitudes $I^{\mu}_{\Gamma_o}$ can be expressed as linear combinations of the bound-bound transition elements, $\langle \varphi_i | r^{\mu} | \varphi_j \rangle$, and bound-free elements $\langle \varphi_i | r^{\mu} | f_{\ell m} \rangle$ and $\langle \varphi_i | r^{\mu} | h^{-}_{\ell m} \rangle$. The former can be extracted from standard molecular property codes and the latter are evaluated by adaptive three-dimensional quadrature. Since the "scattering" orbitals are orthogonal to the target orbitals and the continuum basis functions $f_{\ell m}$ and $h^{-}_{\ell m}$ are orthogonalized to both, this constitutes a strong orthogonality condition between the channel functions $F^{-}_{\Gamma_o\Gamma}$ and the target orbitals; it is entirely equivalent to the Phillips-Kleinman pseudopotentials employed by Lucchese et al.[88] to enforce strong orthogonality.

The strong orthogonality constraint between the channel functions $F_{\Gamma_o\Gamma}$ and the target orbitals $\{\varphi_u\}$ can of course be relaxed by including in the trial function (Eq. (25)) appropriate N-electron penetration terms constructed solely from the target orbitals. The linear coefficients $d^{\Gamma_o}_i$ associated with these terms, or indeed with any other terms one might include in the set $\{\Theta_i\}$ to describe final-state correlation effects, are determined by the variational principle used to construct the Kohn trial function. There is a complication, however, that arises in cases where the target molecule does not possess a center of symmetry. In this case, the penetration terms can be identical to terms used to expand the initial target state Ψ_0. Inclusion of these terms in the expansion for $\Psi^{-}_{\Gamma_o}$ means that the N-electron final state is not necessarily orthogonal to the bound initial state Ψ_0 and that the transition dipole matrix elements we seek in Eq. (82) may be contaminated by introducing a component of the static dipole moment of the target. To remove these errors, we simply orthogonalize the scattering wave function $\Psi^{-}_{\Gamma_o}$ to Ψ_0 before computing the desired photoionization amplitudes. This simply corresponds to a redefinition of the coefficients $d^{\Gamma_o}_i$. This procedure guarantees orthogonality between the initial and final N-electron states

and is an alternative to the strong orthogonality constraint implied by excluding any penetration terms in the expansion of the complex Kohn trial function.

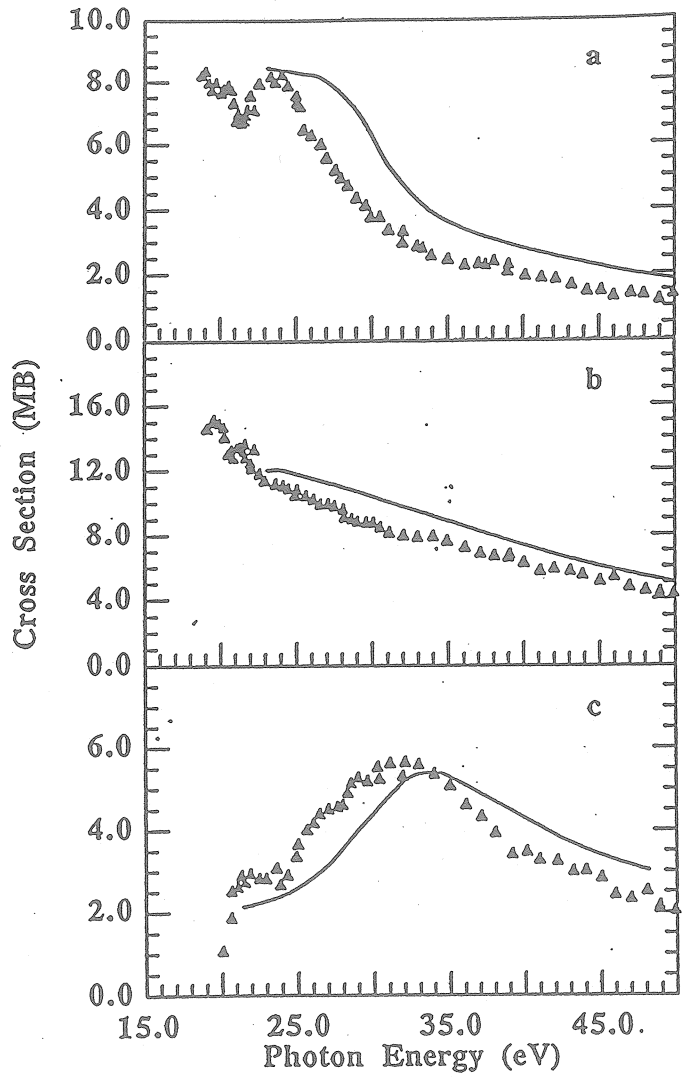

Figure 7. Comparison of present coupled-channel, CI partial cross sections for photoionization of CO with experimental results of Plummer et al. (ref. 89). Panel a: cross sections for production of $X^2\Sigma^+$ state of CO^+. Panel b: cross sections for production of $A^2\Pi$ state of CO^+. Panel c: cross sections for production of $B^2\Sigma^+$ state of CO^+.

We conclude this discussion with an explicit formula for the amplitudes $I_{F_0}^{\mu}$. We can once again characterize these amplitudes as the stationary value of a variational functional[61], as we did in the case of the off-shell T-matrix. This is another example of a specific application of a general class of supervariational principles discussed by Gerjouy et al.[60] The

linear coefficients in the complex Kohn trial function (we use the vector $\underline{c}$ to denote the set of coefficients $\{c_i^{\Gamma_o}\}$, $\{d_i^{\Gamma_o}\}$ and $\{T^{\Gamma_o\Gamma}_{\ell_o m \ell_o m}\}$) are first determined by solving the set of equations.

$$\underline{\underline{M}}_{cc}\underline{c} = -\underline{\underline{M}}_{c\Gamma_o} \tag{88}$$

where M≡H-E, and E is the total energy, ie, $E=E_{target}+\omega$, $\underline{\underline{M}}_{cc}$ is the matrix projection of M onto the space spanned by the functions $A\ (\chi_\Gamma \varphi_i)$, $A\ (\chi_\Gamma h_{\ell m}^{-\Gamma})$ and Θ_i, while Γ_o refers to the functions $A\ (\chi_{\Gamma_o} f_{\ell_o m_o})$. The techniques we use to assemble the various matrix elements required in Eq. (88), including the simplifying use of separable expansions to represent exchange and Q-space interactions, are identical to the procedures employed in our electron-molecule scattering studies. The complex Kohn expression for $I^{\mu}_{\Gamma_o}$ is thus given by

$$I^{\mu}_{\Gamma_o} = \langle \Psi_o | \mu | A \chi_{\Gamma_o} f_{\ell_o} Y_{\ell_o m_o} / r \rangle - \langle \Psi_o | \mu | c \rangle \underline{\underline{M}}^{-1}_{cc} \underline{\underline{M}}_{c\Gamma_o} \tag{89}$$

in cases where $\Psi^-_{\Gamma_o}$ and Ψ_o do not have the same symmetry. When Ψ_o and $\Psi^-_{\Gamma_o}$ do belong to the same irreducible representation, we employ the orthogonalized amplitude

$$\tilde{I}^{\mu}_{\Gamma_o} \equiv I^{\mu}_{\Gamma_o} - \langle \Psi_o | \mu | \Psi_o \rangle \langle \Psi_o | \Psi^-_{\Gamma_o} \rangle \tag{90}$$

as discussed above.

An an illustration of the above formalism, we show in Fig. 7 partial cross sections for photoionization of CO^{35} computed with the complex Kohn method, along with available experimental values[89]. In contrast to previous theoretical studies on this system, these calculations included the effects of interchannel coupling and also employed a correlated ground-state wave function. The dominant effect of interchannel coupling is to remove a spurious $\pi \rightarrow \pi^*$ resonance feature from the continuum that appears at the frozen-core Hartree Fock level. It is also important to combine the effects of final channel coupling with a correlated initial target state to achieve quantitatively correct cross sections.

Dissociative Recombination

There are a number of resonant electron-molecule collisions processes in which the nuclear dynamics must be explicitly treated in order to make contact with experiment. The fixed-nuclei electronic problem can often provide the input necessary to solve the full problem including nuclear dynamics. We will discuss one such application, resonant dissociative recombination of H_3^+. In resonant or 'direct' DR, the electron is captured into a resonance state of the neutral molecule. After capture, the molecule begins to dissociate. During this time, the molecule can autoionize, leaving the ion in a vibrationally or rotationally excited state. Once the resonance curve crosses the ionic curve and becomes bound with respect to the emission of an electron, autoionization can no longer occur, and the system evolves into asymptotic final states. Thus to describe the direct DR process one must know

the energies and widths of the resonant states and describe the dynamics of the dissociative process.

In the application to H_3^+[23], the nuclear dynamics were treated by a wave packet method which involves the direct integration of the time dependent Schrödinger equation:

$$i\hbar\frac{\partial\Psi}{\partial t} = H\Psi \qquad (91)$$

Our calculation was carried out in C_{2v} geometries, thereby restricting the problem to two degrees of freedom. The initial wave function is defined on an (r, R) grid, where r is the H_2 bond distance, and R is the distance from the remaining H to the center of mass of the H_2 bond. The angle between r and R was held fixed at 90°. In these coordinates, the Hamiltonian for the nuclear motion is given by:

$$H(r,R) = -\frac{1}{2\mu_1}\frac{\partial^2}{\partial r^2} - \frac{1}{2\mu_2}\frac{\partial^2}{\partial R^2} + V(r,R) \qquad (92)$$

where μ_1 is the reduced mass of H_2, μ_2 is the reduced mass of $H + H_2$. The potential energy is:

$$V(r,R) = V_0(r,R) + \frac{i\Gamma(r,R)}{2} \qquad (93)$$

where V_0 is the real part of the resonance energy, and $\Gamma(r,R)$ is the complex portion (the resonance width) that describes autoionization[90]. The resonant width and position are determined from fixed-nuclei electron scattering calculations from the H_3^+ ion.

Our treatment of dissociative recombination is a generalization of the time dependent treatment of photodissociation given by Heller[91]. At t=0 the wave packet is defined to be:

$$\begin{aligned}\Psi_0(r,R) &= \sqrt{\frac{\Gamma(r,R)}{2\Pi}}\Phi_0(r,R) \\ &= \sqrt{\frac{\Gamma(r,R)}{2\Pi}}\phi_i(Q_s)\phi_j(Q_b)\end{aligned} \qquad (94)$$

where $\Phi_0(r,R)$ is the initial vibrational wave function on the resonant state surface, which we approximate as the product of harmonic oscillator wave functions, $\phi_i(Q_s)$ and $\phi_j(Q_b)$ in the symmetric stretch and bending normal modes of H_3^+ for each initial vibrational state of interest.

In order to determine the total dissociative recombination cross section, the final wave packet must be projected onto final states[92]. For example, when dissociation produces to an atom and a diatomic one can define:

$$S_2(E) = \sum S_i(E) \qquad (95)$$

where the $S_i(E)$ are the final state probability distributions given by:

$$S_i(E) \propto \left| \iint drdR\chi_i(r)\phi_T(R)\Psi_o(r,R,t) \right|^2 \tag{96}$$

where $\chi_i(r)$ is a vibrational state eigenfunction of the diatomic, and $\phi_T(R)$ is the translation function describing the motion of the atom from the molecular center-of-mass; t is chosen

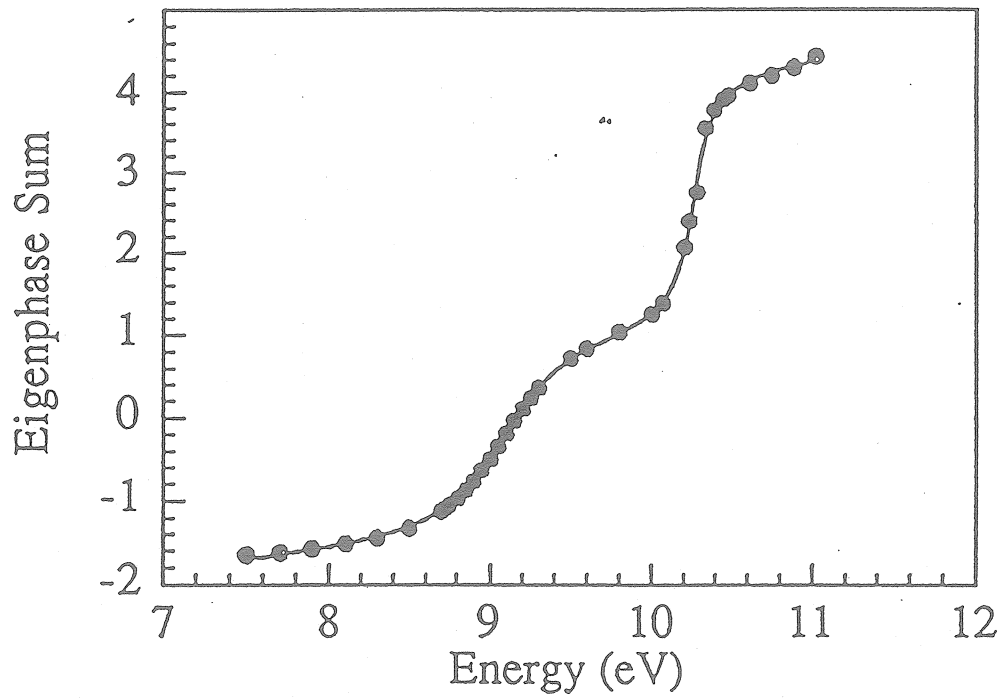

Figure 8 Eigenphase sums for electron H_3^+ scattering at the equilibrium geometry of the ion in A_1 symmetry. Solid circles are the calculated points and theline is the fit of the sum of two Breit-Wigner resonance lineshapes. Rapid jumps by pi in the eigenphase sum indicate resonances.

large enough that the dissociation is complete, i.e.-the fragments are no longer interacting. This expression, when summed over all bound vibrational final states, yields the branching ratio into the two-body channel, $S_2(E)$. Once the sum in Eq. (95) is extended to include the continuum H_2 states the result is the total dissociation cross section.

The ground state equilibrium geometry of H_3^+ is an equilateral triangle, (D_{3h} symmetry) with bond lengths 1.65 a_0[93]. The electronic configuration is $1a_1'^2$. The resonance states correspond to the capture of an electron into the low-lying doubly degenerate e´orbital, with the simultaneous promotion of one of the a_1' electrons to the same orbital:

$$H_3^+(1a_1'^2) + e^- \rightarrow H_3(1a_1'1e'^2)$$

Because of the degeneracy of the doubly occupied orbital, four distinct molecular configurations are possible. We carried out complex Kohn calculations to map out the four resonance potential energy surfaces from the Franck-Condon region to the points where they cross into the bound state manifolds. The eigenphase sums were fit to a Breit-Wigner form to obtain the resonance widths and positions. An example is shown in Fig. 8.

In Fig. 9 we show the individual contributions of the four resonance states and the total DR cross section as a function of impact energy compared to experiment. These results are in quantitative agreement, both for the position of the peak and its shape and magnitude, with the ~ 9 eV peak reported by high energy cross section measured by Larsson et al[94].

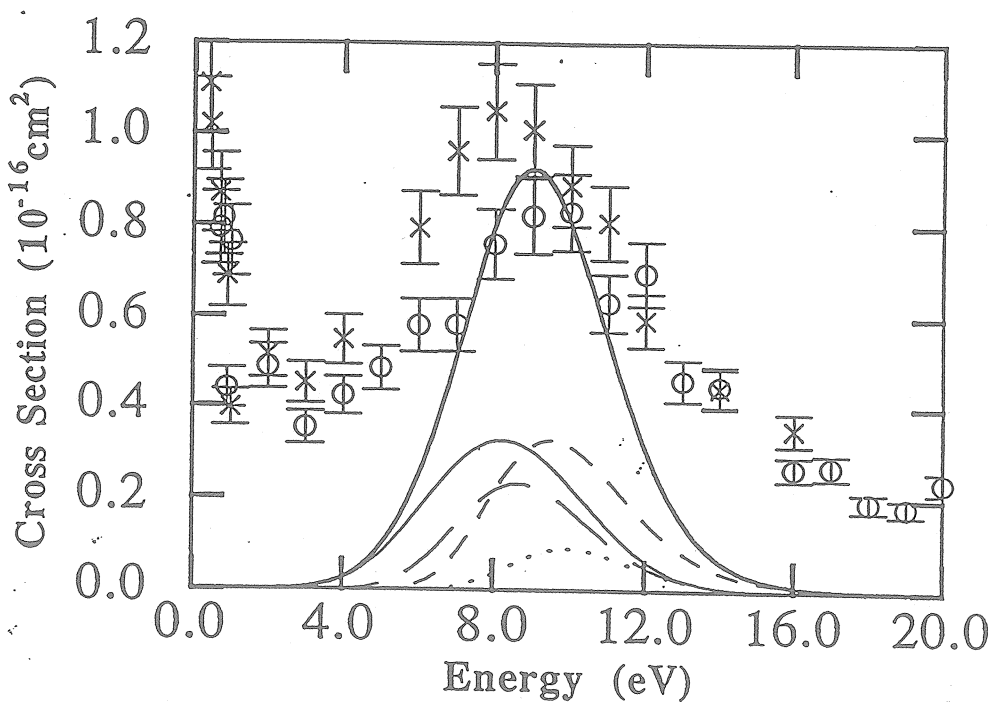

Figure 9. Total (heavy solid line and partial resonance DR cross sections as functions of incident electron energy: 1^2A_1 (solid line), 1^2B_2 (long dashed line), 2^2A_1 (medium dashed line) and 2^2B_2 (short dashed line). The experimental results are those of Larsson et al.[94]

Acknowledgement

This work was performed under the auspices of the U.S. Department of Energy by Lawrence Livermore National Laboratory under contract number W-7405-Eng-48. AEO wishes to acknowledge support from the National Science Foundation.

REFERENCES

1. A. B. Ehrhardt and W. D. Larger, *Collisional Processes of Hydrocarbons in Hydrogen Plasmas*, PPPL-2477 (Sept. 1987).
2. A. Gallagher, "Materials Issues in Amorphous-Semiconductor Technology Symposium," Palo Alto, 1986 (Mater. Res. Soc., Pittsburgh, PA1986), p. 3.
3. J. B. A. Mitchell, Phys. Repts. 186, 216 (1990).
4. M. A. Biondi, in *Principles of Laser Plasmas*, ed. by G. Bekefi (Wiley, New York, 1976) p. 125.
5. See, for example, *Excimer Lasers,* ed. by C. K. Rhodes (Springer-Verlag, New York, 1979).
6. A. Dalgarno and J. H. Black, Rep. Prog. Phys., 39, 573 (1976).
7. For a recent review, see D. R. Bates, M. F. Guest and R. A. Kendall, Planet. Space Sci. 41, 9 (1993).
8. J. Z. H. Zhang and W. H. Miller, J. Chem. Phys. 91, 1528 (1989).
9. T.Kato, Prog. Theo. Phys. 6, 394 (1951).
10. W. Kohn, Phys. Rev. 74, 1763 (1948).
11 R. K. Nesbet, *Variational Methods in Electron-Atom Scattering Theory* (Plenum, New York, 1980).
12. R. K. Nesbet, Phys. Rev. 175, 134 (1968); 179, 60 (1969).
13. Y. Mito and M. Kamimura, Prog. Theo. Phys. 56, 583 (1976).
14. W. H. Miller and B. M. D. D. Jansen op de Haar, J. Chem Phys. 86, 6213 (1987).
15. C. W. McCurdy, T. N. Rescigno and B. I. Schneider *Phys. Rev. A* 36, 2061 (1987).
16. T. N. Rescigno and B. I. Schneider, Phys. Rev. A 37, 1044 (1988).
17. C. W. McCurdy and T. N. Rescigno, Phys. Rev. A 39, 4487 (1989).
18. A. D. Becke, J. Chem. Phys. 88, 2547 (1988).
19. T. N. Rescigno, B. H. Lengsfield III and C. W. McCurdy, in *Modern Electronic Structure*, edited by D. Yarkony (World Scientific, 1994).
20. J. N. Bardsley, in *Electron-Molecule and Photon-Molecule Collisions,* edited by T. N. Rescigno, V. McKoy and B. I. Schneider (Plenum, New York, 1979), p. 267
21. M. A. Morrison, Adv. At. Molec. Phys. 24, 51 (1988).
22. A. U. Hazi, T. N. Rescigno and M. Kurilla, Phys. Rev. A 23, 1089 (1981); A. U. Hazi, A. E. Orel and T. N. Rescigno, Phys. Rev. Letts. 46, 918 (1981).
23. A. E. Orel and K. C. Kulander, Phys. Rev. Letts. 71, 4315 (1993).
24. P. G. Burke, *Potential Scattering in Atomic Physics,* (Plenum, New York, 1977).
25. M. Abramowitz and I. A. Stegun, *Handbook of Mathematical Functions*, (Dover, New York, 1965).
26. D. Lyons and R. K. Nesbet, J. Comp. Phys. 11, 166 (1973);R. L. Smith and D. G. Truhlar, Comp. Phys. Commun. 5, 80 (1973); J. Abdallah and D. G. Truhlar, *ibid.* 9, 327 (1975).
27. T. N. Rescigno and A. E. Orel, Phys. Rev. A 43, 1625 (1991).

28. Y. Sun, D. J. Kouri, D. G. Truhlar and D. W. Schwenke, Phys. Rev. A 41, 4857 (1990).
29. B. I. Schneider and T. N. Rescigno, Phys. Rev. A 37, 3749 (1988).
30. A. E. Orel. T. N. Rescigno and B. H. Lengsfield III, Phys. Rev. A 44, 4328 (1991).
31. B. H. Lengsfield III, T. N. Rescigno and C. W. McCurdy, *Phys. Rev. A* 44, 4296 (1991).
32. B. H. Lengsfield III and T. N. Rescigno, Phys. Rev. A 44, 2913 (1991).
33. H. E. Saraph, M. J. Seaton and J. Shemming, Proc. Phys. Soc. London 89, 27 (1966).
34. P. G. Burke, A. Hibbert and W. D. Robb, J. Phys. B 4, 153 (1971).
35. T. N. Rescigno, B. H. Lengsfield III and A. E. Orel, J. Chem. Phys. 99, 5097 (1993).
36. H. Feshbach, Ann. Phys. (N. Y.) 5, 357 (1958); 19, 287 (1962).
37. B. H. Lengsfield III and B. Liu, J. Chem. Phys. 75, 478 (1981).
38. J. A. Pople, R. Krishnam, H. B. Schlegel and J. S. Binkley, Int. J. Quan. Chem. Symp. 13, 225 (1979).
39. E. R. Davidson, J. Comp. Phys. 17, 87 (1975); P. E. M. Siegbahn, J. Chem. Phys. 70, 5391 (1980); 72, 1647 (1980).
40. T. N. Rescigno and A. E. Orel, Phys. Rev. A 23, 1134 (1981); 24, 1267 (1981); B. Gyarmati, A. T. Kruppa and J. Revai, Nucl. Phys. A 326, 119 (1979).
41. C. W. Murray, N. C. Handy and G. J. Laming, Molec. Phys. 78, 997 (1993).
42. J. D. Jackson, *Classical Electrodynamics,* (Wiley, New York, 1962), p. 69.
43. A. D. Becke and R. M. Dickson, J. Chem. Phys. 89, 2993 (1988).
44. W. Eissner and M. J. Seaton, J. Phys. B 5, 2187 (1972).
45. R. K. Nesbet, Comp. Phys. Comm. 6, 275 (1973).
46. P. G. Burke, Comp. Phys. Comm. 6, 288 (1973).
47. S. Chung and C. C. Lin, Phys. Rev. A 17, 1874 (1978).
48. C. Weatherford, Phys. Rev. A 22, 2519 (1980).
49. A. E. Orel, T. N. Rescigno and B. H. Lengsfield, Phys. Rev. A 42, 5292 (1990).
50. T. N. Rescigno and B. I. Schneider, Phys. Rev. A 45, 2894 (1992).
51. T. N. Rescigno, "Low energy electron collision processes in molecular chlorine", Phys. Rev. A XX,xxxx (1994)
52. T. J. Gil, C. W. McCurdy, T. N. Rescigno and B. H. Lengsfield III, Phys. Rev. A 47, 255 (1993).
53. D. E. Golden, N. F. Lane, A. Temkin and E. Gerjuoy, Rev. Mod. Phys. 43 642 (1971)
54. M. A. Morrison, Adv. Atom. Mol. Phys. 24, 51 (1988)
55. A. M. Arthurs and A. Dalgarno, Proc. R. Soc. A 256, 540 (1960).
56. N. Chandra and A. Temkin , Phys. Rev. A 13, 188 (1976).
57. M. Shugard and A.U. Hazi, Phys. Rev. A 12, 1895 (1975).

58. M.A. Morrison, J. Phys. B 19, L707 (1986); M.A. Morrison, M. Abdolsalami and B. K. Elza, Phys. Rev. A 43, 3440 (1991); B. K. Elza, University of Oklahoma, PhD Thesis, (1992,unpublished).
59. R. G. Newton, *Scattering Theory of Waves and Particles*, (McGraw-Hill, New York, 1966), p.188.
60. E. Gerjouy, A. Rau and L. Spruch, J. Math. Phys. 13, 1797 (1972).
61. A. E. Orel and T. N. Rescigno, Phys. Rev. A 41, 1695 (1990).
62. D. M. Chase, Phys. Rev. 104, 838 (1956).
63. T. N. Rescigno, B. K. Elza and B. H. Lengsfield III, J. Phys. B 26, L567 (1993).
64. M.J. Brunger, S.J. Buckman, D.S. Newman and D.T. Alle, J. Phys. B 24, 1435 (1991).
65. J.P. England, M.T. Elford and R.W. Crompton, Aust. J. Phys. 41, 573 (1988).
66. S.J. Buckman, M.J. Brunger, D.S. Newman, G. Snitchler, S. Alston, D.W. Norcross, M.A. Morrison, B.C. Saha, G. Danby and W.K. Trail, Phys. Rev. Letts. 65, 3253 (1990).
67. F. Linder and H. Schmidt, Z. Naturforsch. 26a, 1603 (1971).
68. H. Ehrhardt, L. Langhans, F. Linder and H.S. Taylor, Phys. Rev. 173, 222 (1968).
69. K. Rohr and F. Linder, J. Phys. B 9, 2521 (1976).
70. L. A. Morgan and P. G. Burke, J. Phys. B 21, 2091 (1988); G. Snitchler, D. Norcross, A. Jain and S. Alston, Phys. Rev. A 42, 671 (1990).
71. K. Rohr, J. Phys. B 13, 4897 (1980).
72. W. Sohn, K. Jung and H. Ehrhardt, J. Phys. B 16, 891 (1983).
73. T. N. Rescigno, A. E. Orel and C. W. McCurdy (unpublished).
74. W. Sohn, K. H. Kochem, K. M. Scheuerlein, K. Jung and H. Ehrhardt, J. Phys. B 19, 3625 (1986).
75. O. H. Crawford, A. Dalgarno and P. B. Hays, Molec. Phys. 13, 181 (1967).
76. W. R. Garrett, Molec. Phys. 24, 465 (1972).
77. See, for example, N. F. Lane, Rev. Mod. Phys. 52, 29 (1980).
78. M. E. Rose, *Elementary Theory of Angular Momentum* (Wiley, New York ,1967) pp. 62-65.
79. See, for example, M. J. Seaton, Proc. Phys. Soc. London 79, 1105 (1962).
80. See, for example, L. A. Collins and D. W. Norcross, Phys. Rev. A 18, 467 (1978). This paper gives a clear treatment of the subject and also contains many references to earlier work.
81. D. W. Norcross and N. T. Padial, Phys. Rev. A 25, 226 (1982).
82. T. N. Rescigno and B. H. Lengsfield III, Z. Phys. D 24, 117 (1992).
83. T. N. Rescigno, B. H. Lengsfield III, C. W. McCurdy and S. D. Parker, Phys. Rev. A 45, 7800 (1992).
84. B. H. Lengsfield III and T. N. Rescigno, (unpublished).
85. R. J. Gulley, M. J. Brunger and S. A. Buckman, Phys. B 26, 2913 (1993).

86. R. R. Lucchese and V. McKoy, Phys. Rev. A 24, 770 (1981); R. R. Lucchese, G. Raseev and V. McKoy, Phys. Rev. A 25, 2572 (1982).
87. J. C. Tully, R. S. Berry and B. J. Dalton, Phys. Rev. 176, 95 (1968).
88. B. Basden and R. R. Lucchese, Phys. Rev. A 37, 89 (1988).
89. E. W. Plummer, T. Gustafsson, W. Gudat and D. E. Eastman, Phys. Rev. A 15, 2339 (1977).
90. C. W. McCurdy and J. L. Turner, J. Chem. Phys. 78, 6773 (1983).
91. E. J. Heller, J. Chem. Phys. 68, 3891 (1978).
92. K. C. Kulander and E. J. Heller, J. Chem. Phys. 69, 2439 (1978).
93. G. Herzberg, *Electronic Spectra of Polyatomic Molecules*, (Van Nostrand Reinhold Company, New York), pg. 289 (1966).
94. M. Larssen, H. Danared, J. R. Mowat, P. Sigray, G. Sundström, L. Broström, A. Filevich, A. Källberg, S. Mannervik, K. G. Rensfelt and S. Datz, Phys. Rev. Lett.